

The interaction of radiation with matter

Myroslav Kavstyuk

KVI – Center for Advanced Radiation Technology

m.kavatsyuk@rug.nl



university of
groningen

kvi - center for advanced
radiation technology

Radiation categories

charged particles

neutral particles

heavy charged particles

high-energy photons

fast electrons

neutrons

neutrinos

“Coulomb”
“easily stopped”



Nomenclature high-energy photons

- high-energy photons = energy higher than ionisation energies, so roughly $>1 \text{ keV}$ ($\lambda < 1 \text{ nm}$)
- in principle:
 - X-rays: atomic transitions
 - up to $\sim 115 \text{ keV}$ for uranium
 - γ -rays: nuclear transitions
 - from few eV to many MeV
- other sources of high-energy photons
 - bremsstrahlung
 - synchrotron radiation
 - annihilation radiation
- to keep things simple: “ γ -rays”

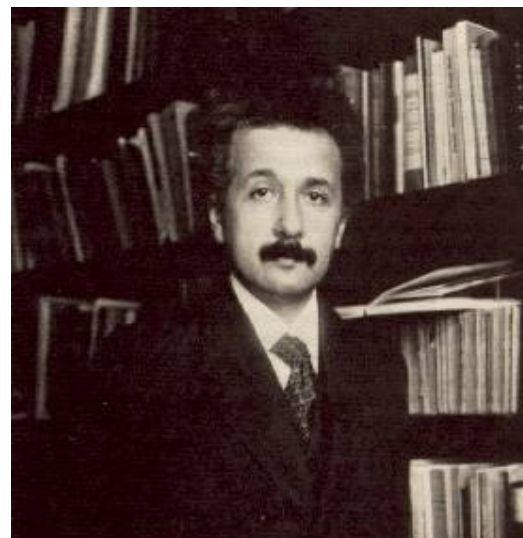
High-energy photons: 3 major interactions

- photo-electric effect
- Compton scattering
- pair production

Nobel prizes in physics



1921



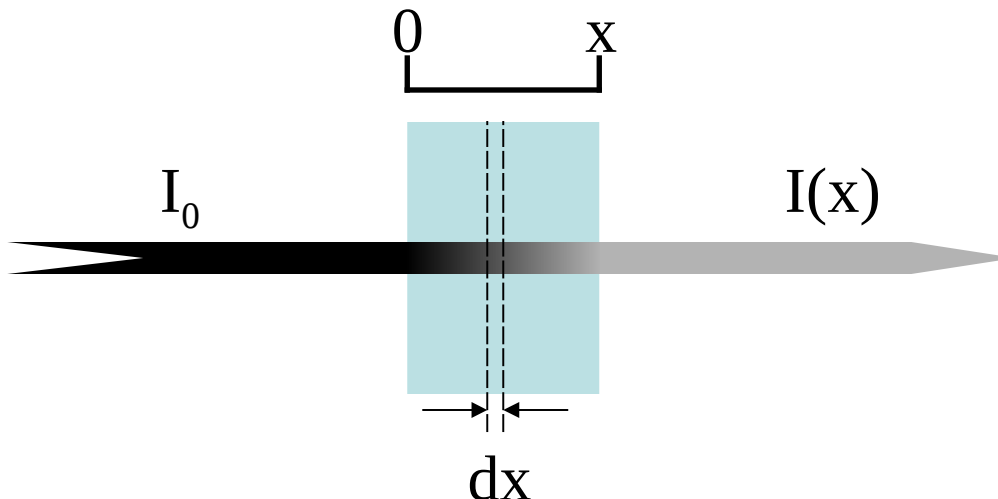
Albert Einstein

1927



Arthur H. Compton

Attenuation of gamma rays (1/2)



all-or-nothing processes: $\frac{dI}{dx} \propto \mu I$ $\frac{dI(x)}{dx} = -\mu I(x)$

μ : linear attenuation coefficient

$$I(x) = I_0 e^{-\mu x}$$

Attenuation of gamma rays (2/2)

mean free path

$$\lambda = \frac{\int_0^\infty x e^{-\mu x} dx}{\int_0^\infty e^{-\mu x} dx} = \frac{1}{\mu}$$

mass attenuation coefficient

$$\mu_\rho \equiv \frac{\mu}{\rho}$$

$$\mu \left[\frac{1}{\text{cm}} \right], \rho \left[\frac{\text{g}}{\text{cm}^3} \right] \rightarrow \mu_\rho \left[\frac{\text{cm}^2}{\text{g}} \right]$$

half-thickness

$$I(x) = I_0 e^{-\ln 2 \frac{x}{d_{1/2}}}$$

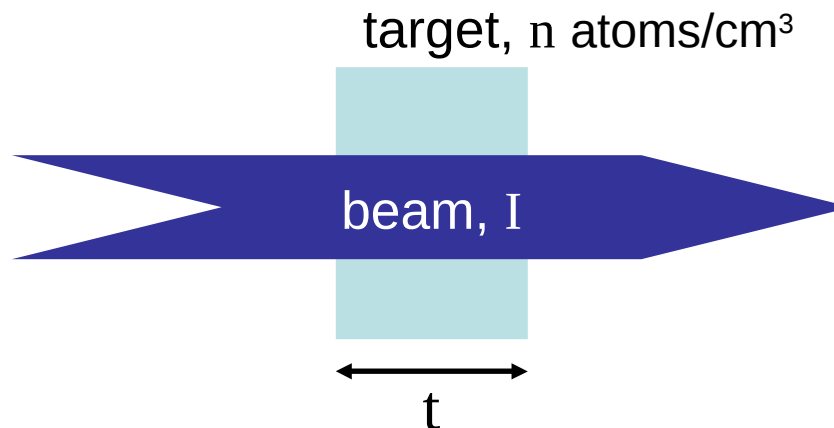
$$d_{1/2} = \frac{\ln 2}{\mu} \left[\text{cm or } \frac{\text{g}}{\text{cm}^2} \right]$$

compound or mixture

$$\left(\frac{\mu}{\rho} \right)_c = \sum_i w_i \left(\frac{\mu}{\rho} \right)_i$$

w_i : weight fraction of element i

Interaction cross section



number of “interactions” proportional with:

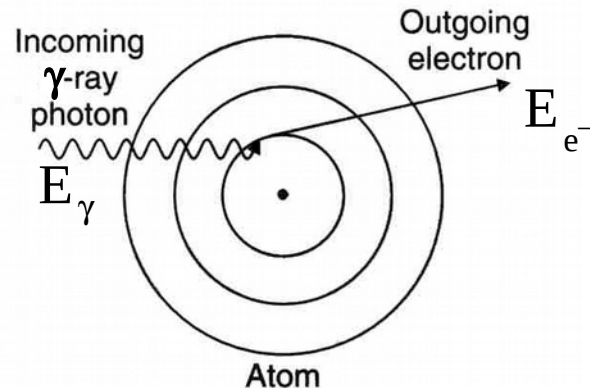
- beam intensity I [1/s]
- number of “reaction partners” encountered $n t (\equiv t')$ [cm^2]

$$N = \sigma I t'$$

σ = cross section [cm^2]

1 barn (b) = 10^{-24} cm^2

Photo-electric effect



- interaction with whole atom
- K-electron most probable
- energy deposition:
 - $E_{e^-} = E_\gamma - E_b$ (E_b : electron binding energy) $\rightarrow E_\gamma > E_b$
 - electron cloud is “rearranged”:
 - X-rays
 - Auger electrons
 - photo-electron preferentially emitted in a forward direction

Photo-electric cross section in lead

absorption
edges

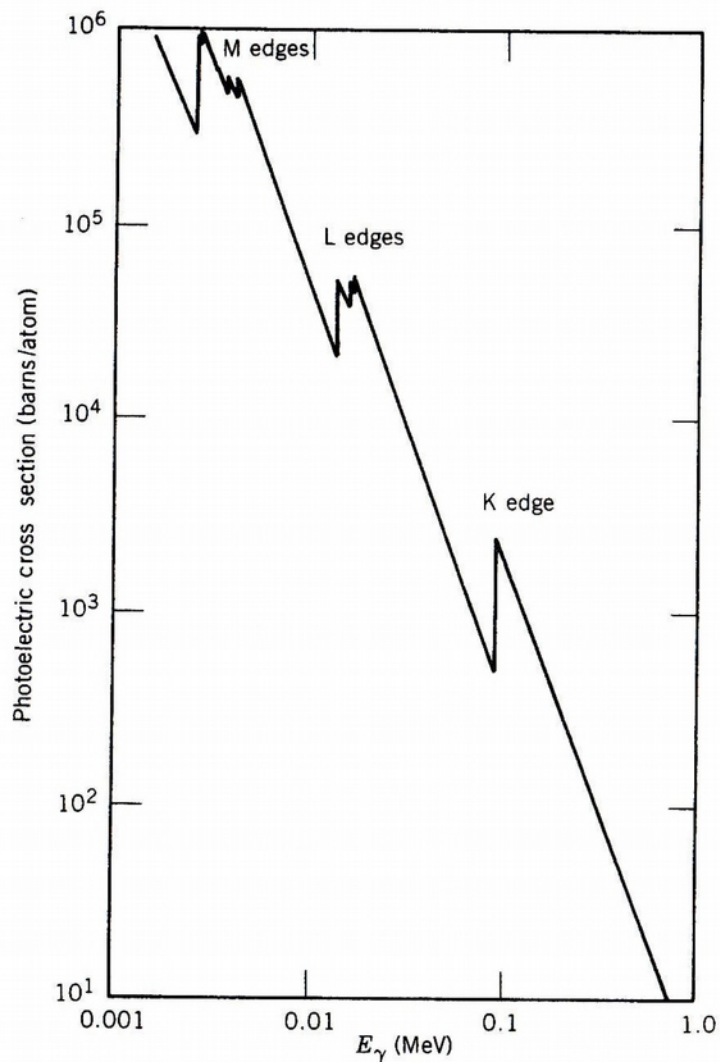
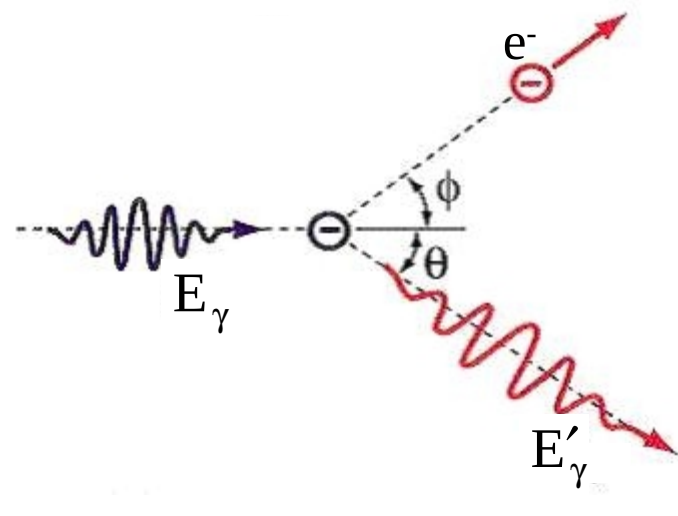


Figure 7.5 Photoelectric cross section in Pb. The discrete jumps correspond to the binding energies of various electron shells; the K-electron binding energy, for example, is 88 keV. To convert the cross section to the linear absorption coefficient τ in cm^{-1} , multiply by 0.033.

Compton scattering (1/2)



$$E'_\gamma = \frac{E_\gamma}{1 + \frac{E_\gamma}{m_0 c^2} (1 - \cos \theta)}$$

$m_0 c^2$: electron rest mass (511 keV)
 θ : scattering angle

Compton scattering (2/2)

angular distribution: Klein-Nishina formula

$$\frac{d\sigma}{d\Omega}(\theta) = \frac{1}{2} r_e^2 \left(\frac{E'_\gamma}{E_\gamma} \right)^2 \left(\frac{E_\gamma}{E'_\gamma} + \frac{E'_\gamma}{E_\gamma} - \sin^2 \theta \right) \quad \left[\frac{\text{cm}^2}{\text{sr}} \right]$$

$$\frac{d\sigma}{d\Omega}(\theta) = \frac{1}{2} r_e^2 \left(\frac{1}{1 + \alpha(1 - \cos \theta)} \right)^2 \left(1 + \cos^2 \theta + \frac{\alpha^2 (1 - \cos \theta)^2}{1 + \alpha(1 - \cos \theta)} \right) \quad \left[\frac{\text{cm}^2}{\text{sr}} \right]$$

$$\alpha = \frac{E_\gamma}{m_0 c^2}$$

r_e : classical electron radius = $2.82 \times 10^{-13} \text{ cm}$

Compton scattering

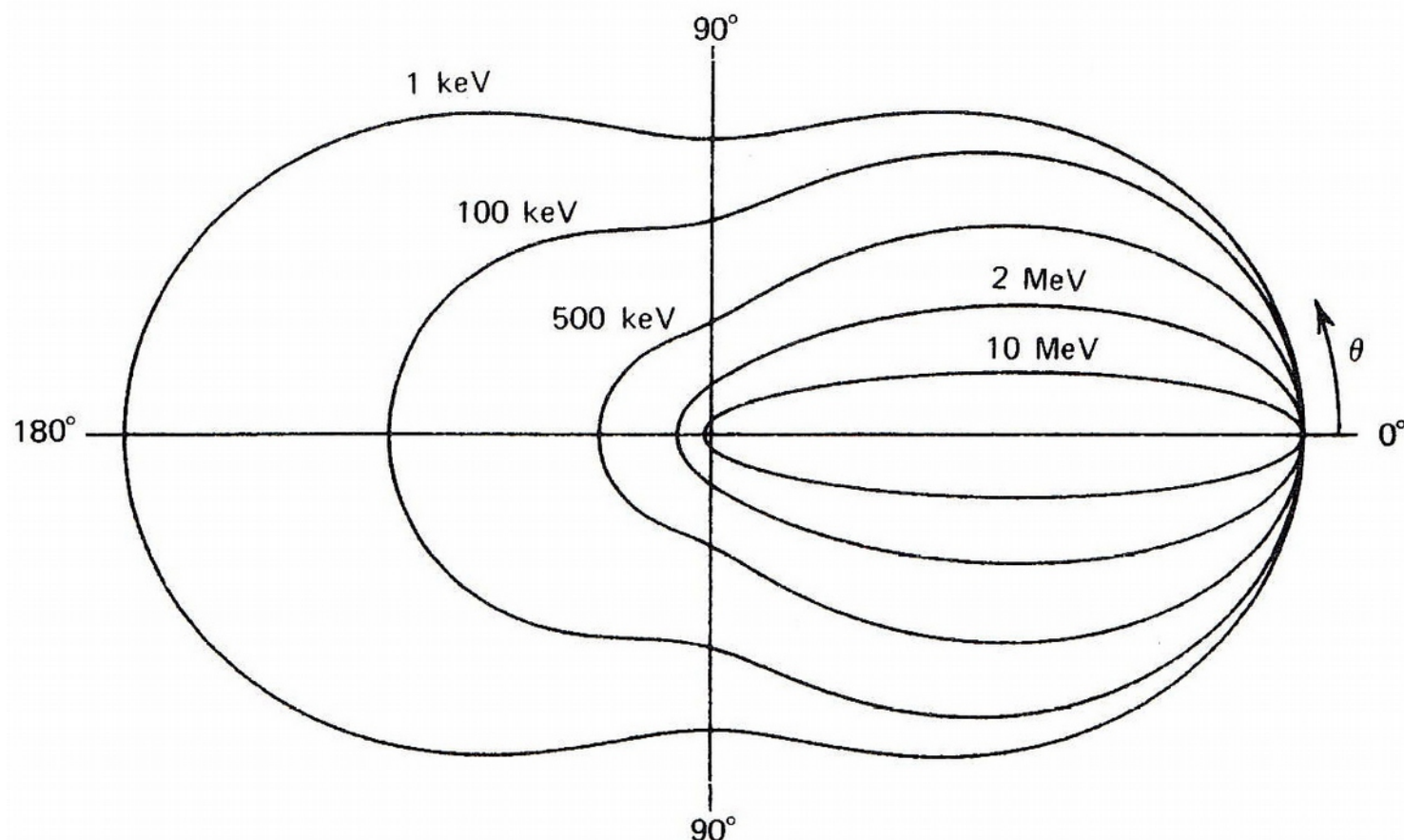


Figure 2.19 A polar plot of the number of photons (incident from the left) Compton scattered into a unit solid angle at the scattering angle θ . The curves are shown for the indicated initial energies.

Compton scattering

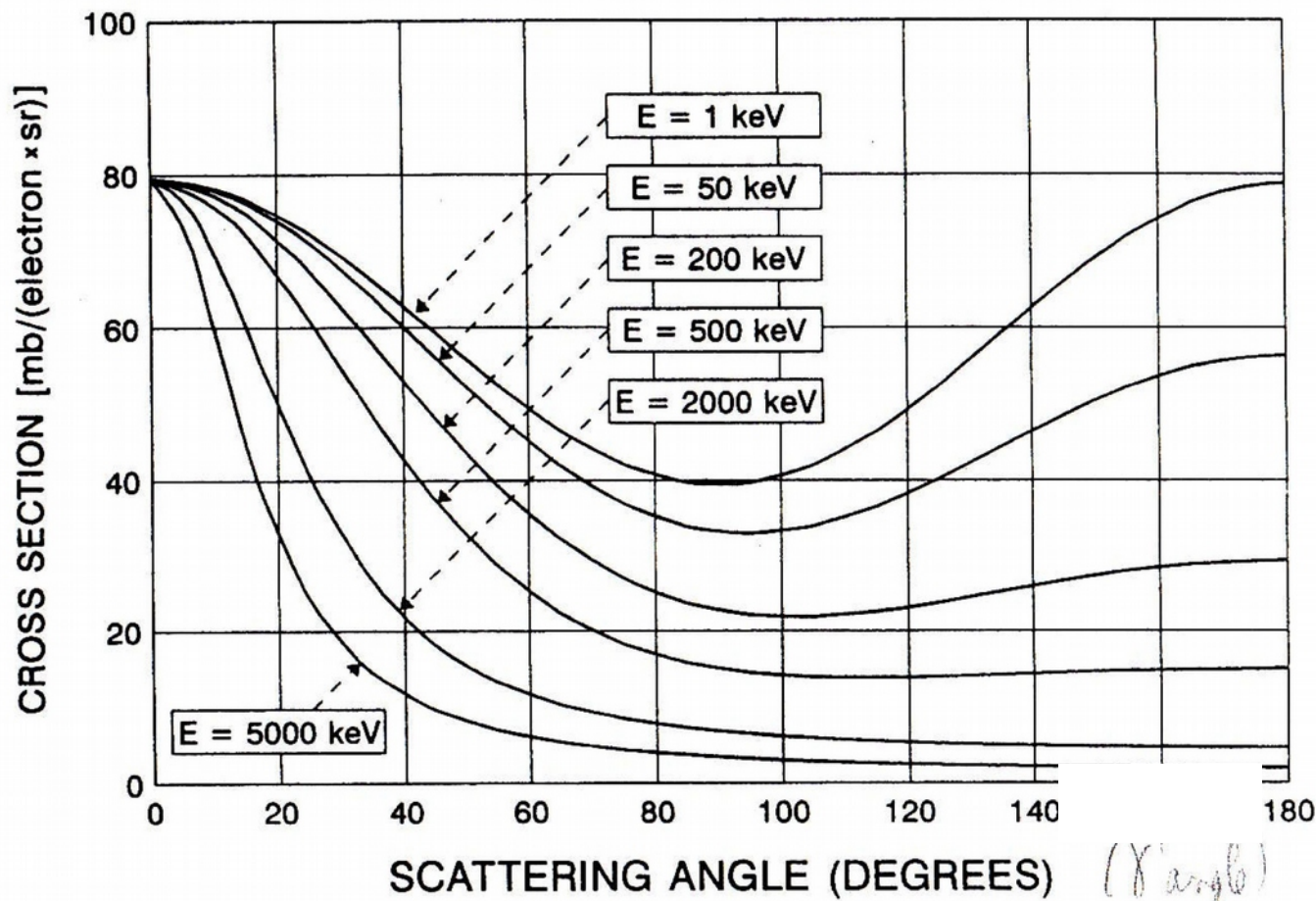


Figure 7-3 Differential cross-section for Compton scattering (=the number of photons scattered into a solid angle at a mean scattering angle ϑ). This figure implies a very strong forward-peaking angular distribution for the most energetic photons; see also Fig. 7-4 and the text, which give a less elusive picture of this point.

Compton scattering

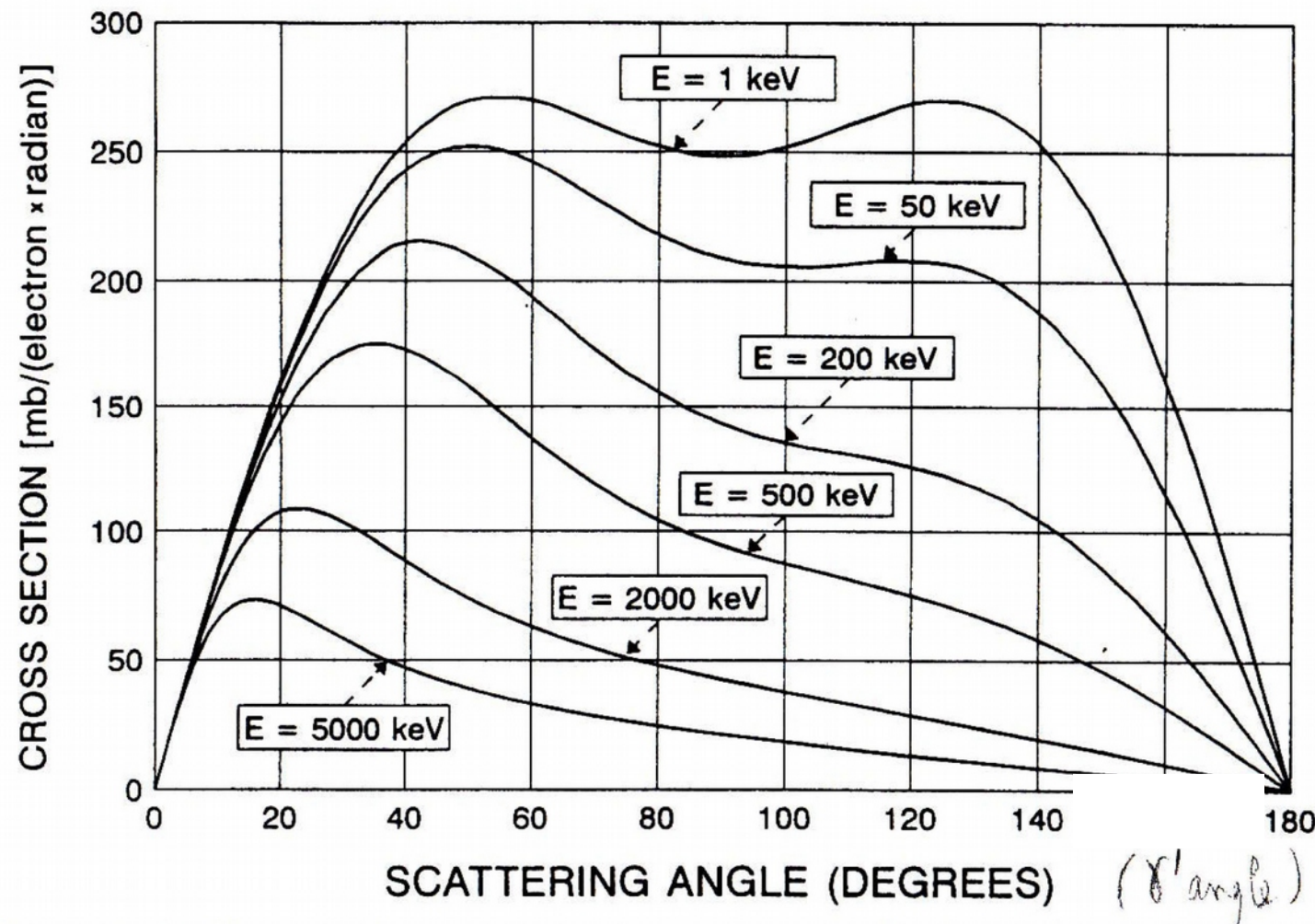
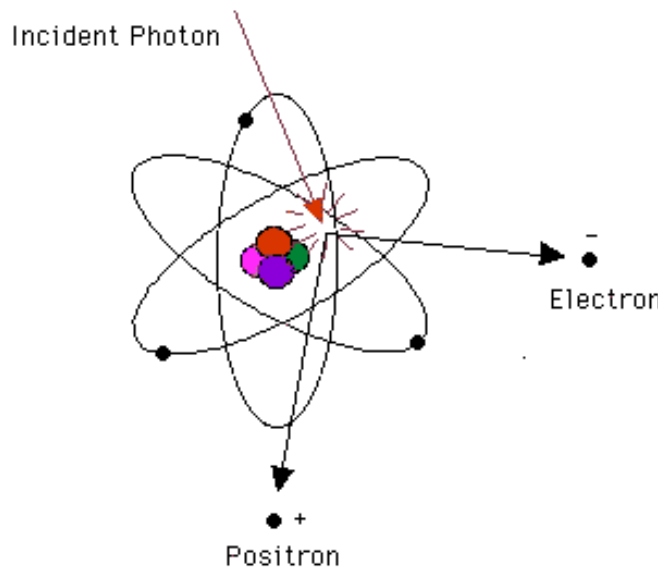
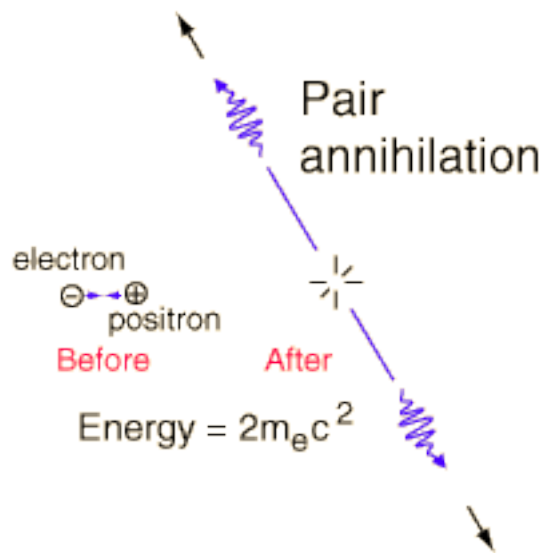


Figure 7-4 Cross-section per unit scattering angle (=number versus angle distribution) of the Compton-scattering process, for some primary gamma-ray energies.

Pair production



- nucleus for momentum conservation
- requires $E_\gamma > 2 m_0 c^2 = 1022 \text{ keV}$
- kinetic energy $(e^- + e^+) = E_\gamma - 1022 \text{ keV}$
- e^+ annihilates with an electron
 - two 511 keV annihilation photons
 - emitted back-to-back



Dependence on atomic number and energy

type of interaction	attenuation coefficient	comment
photo-electric effect	$\tau \propto \mu Z^{4.5} E_g^{-3.5}$	dominates for low energies and heavy elements
Compton scattering	$\sigma \propto \mu Z E_g^{-1}$ (0.1 to 10 MeV)	dominates from ~0.5 to 5 MeV (for most elements)
pair production	$\kappa \propto \mu Z^2 (E_g - 1022 \text{ keV})$	E close to 1 MeV
	$\kappa \propto \mu Z^2 \ln(E_g)$	$E \gg 1 \text{ MeV}$ dominates for high energies and heavy elements

Z : atomic
number

Dominant interaction vs. energy and atomic number

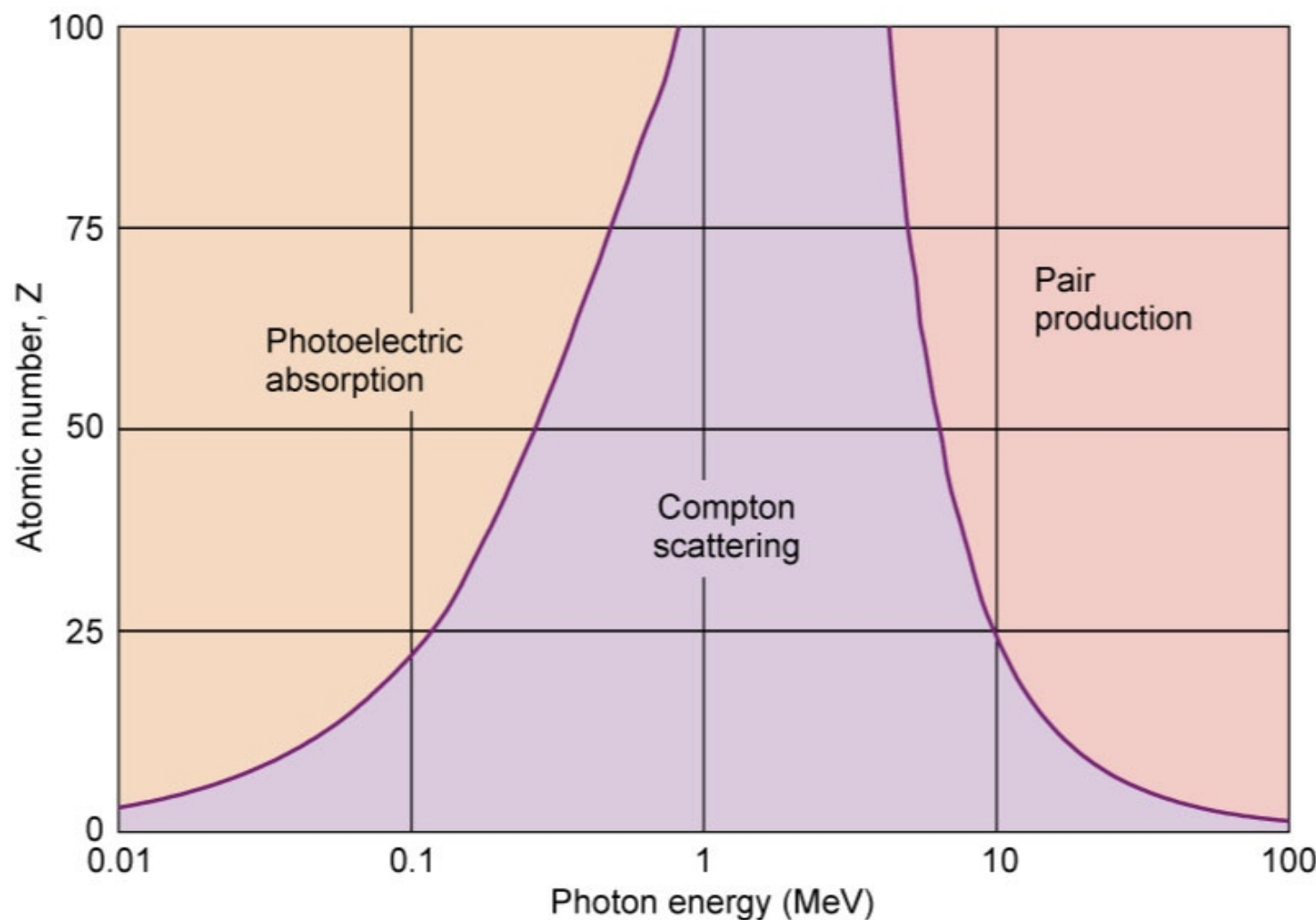


Fig. 6-18 Predominating (most probable) interaction versus photon energy for absorbers of different atomic numbers. Curves were generated using values obtained from reference 2.

Copyright © 2012, 2003, 1987, 1980 by Saunders, an imprint of Elsevier Inc.

Total γ -ray attenuation

$$\mu = \tau + \sigma + \kappa$$

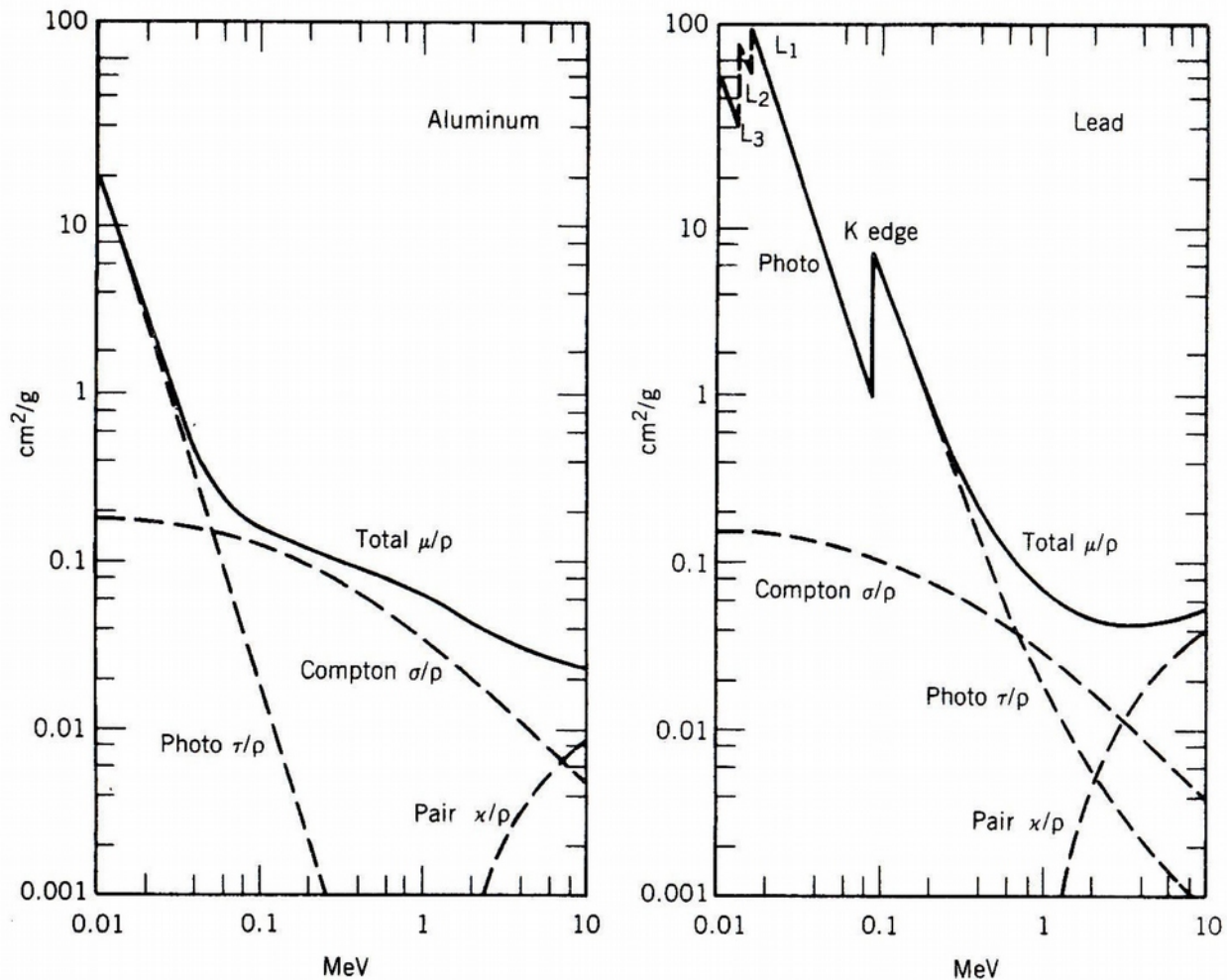


Figure 7.10 Photon mass attenuation coefficients, equal to the linear attenuation coefficients divided by the density (to suppress effects due simply to the number of electrons in the material) for the three processes in Al and Pb.

Half-thickness

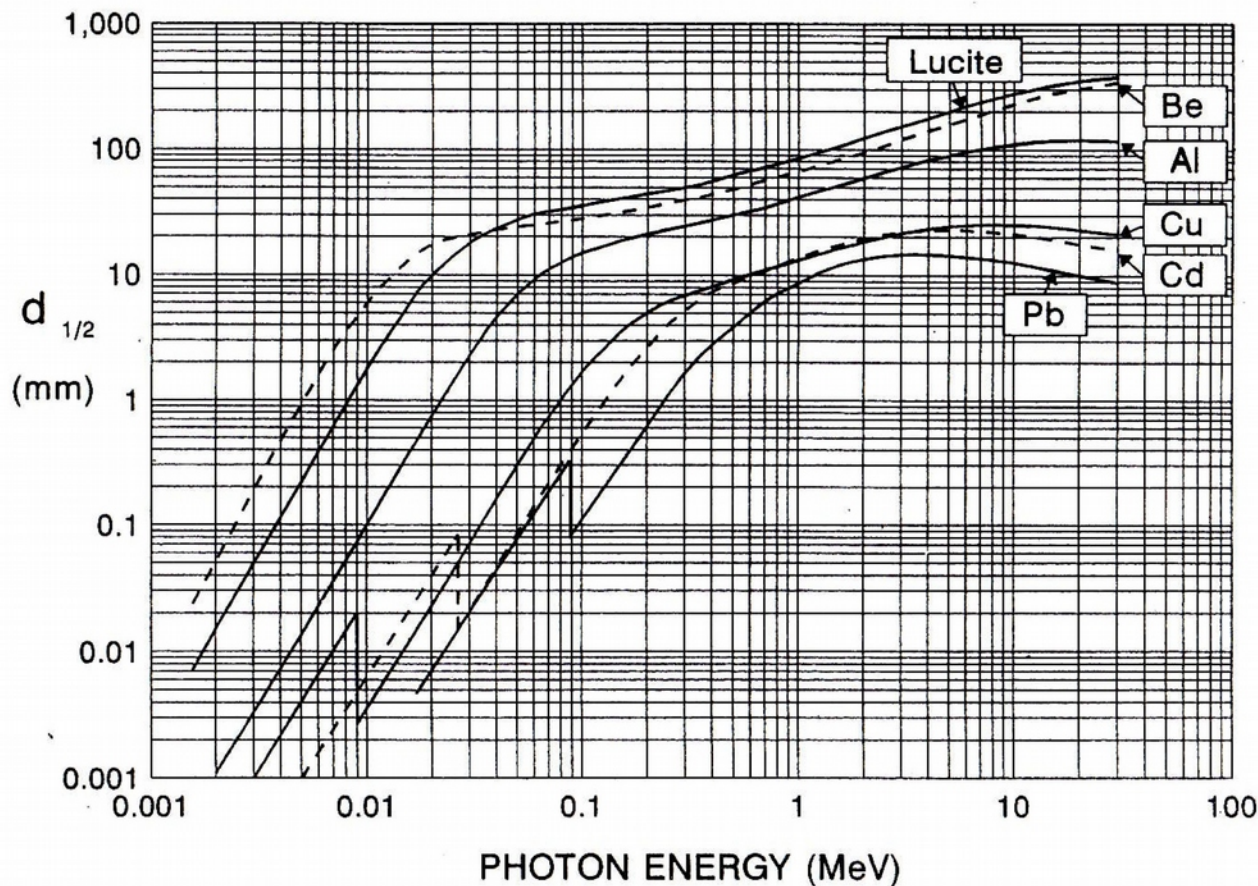


Figure 7-7 Half-thicknesses (in mm) for some frequently used absorber materials computed with the present procedure. The lead curve is not extended below 20 keV, because of the vicinity of the L_I absorption edge. The accuracy of these curves is in practice the reading accuracy. "Lucite" (polymethyl methacrylate) is also called "Perspex" or Plexiglass".

Heavy charged particles

- protons, alpha particles, atomic ions
- primary interaction through Coulomb forces
(only at low energy, nuclear reactions are important for energy loss)
- Coulomb scattering by atomic electrons
 - maximum energy transfer (head-on collision)

$$\Delta E_{\max} \approx E \frac{4m}{M}$$

m: electron mass
M: mass heavy particle

for 10 MeV proton: $\Delta E_{\max} \approx 20 \text{ keV}$

- energy loss in very many small steps
- Coulomb force has infinite range, so interaction with many electrons simultaneously
 - continuous, gradual, energy loss

Heavy charged particles

- Coulomb interaction leads to:
 - electron capture/loss by projectile
 - excitation projectile
 - excitation and ionisation of target atoms
 - basis for detection
- kinetic energy is transferred to δ -rays, X-rays, Auger electrons, ...
- many-faceted and complicated process
- paths are essentially straight because
 - $M \gg m_e$
→ per interaction a small deflection
 - interactions in all directions

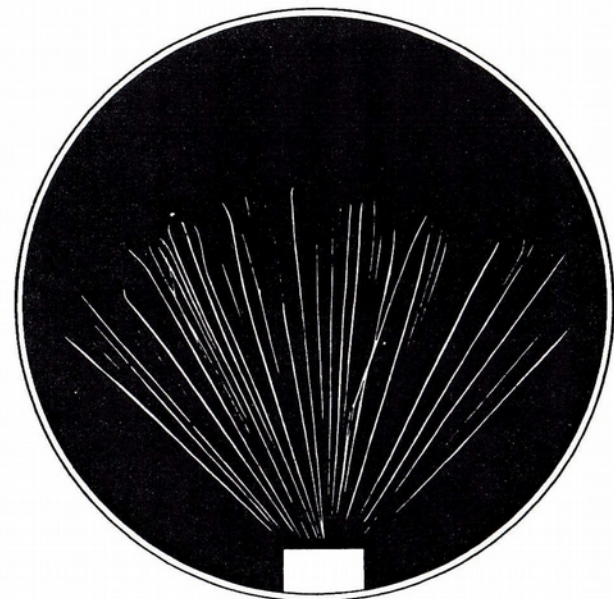
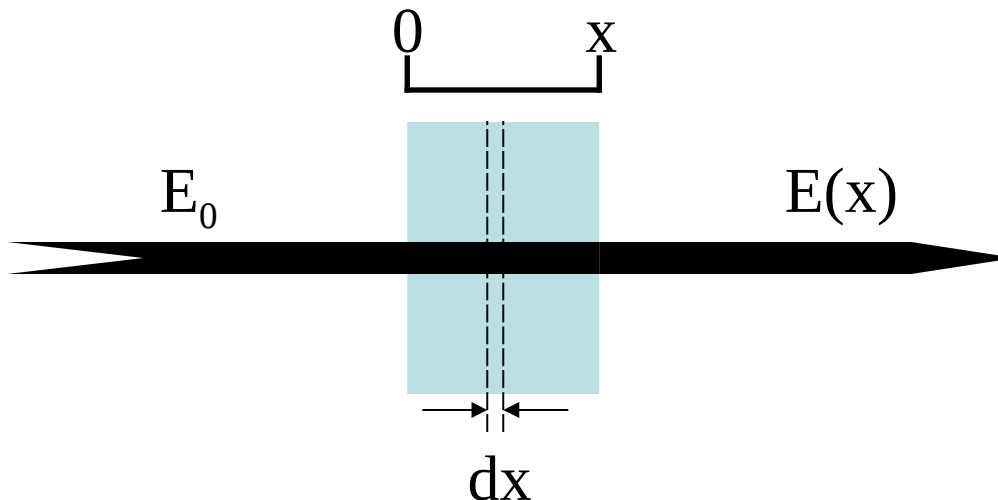


Figure 7.1 Cloud chamber tracks of α particles from the decay of ^{210}Po .

Stopping power



- stopping power \equiv energy loss per unit of amount of material

- linear stopping power

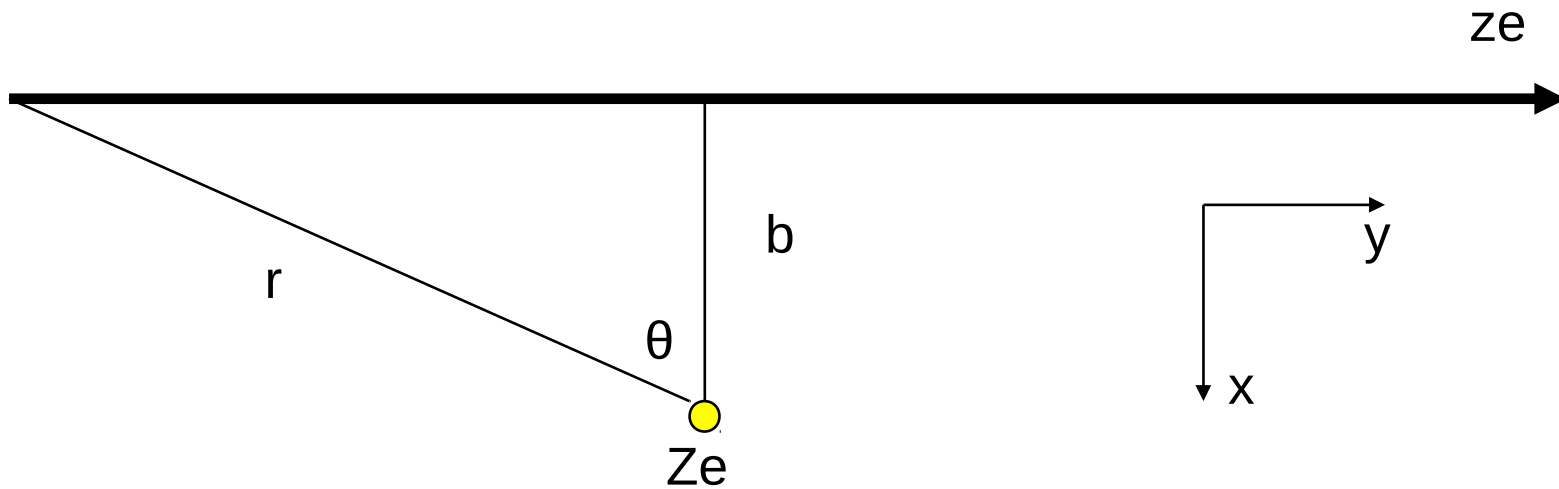
$$S = -\frac{dE}{dx} \quad \left[\text{e.g. } \frac{\text{MeV}}{\text{cm}} \right]$$

- specific stopping power

$$S = -\frac{dE}{d(\rho x)} \quad \left[\text{e.g. } \frac{\text{MeV}}{\text{g/cm}^2} \right]$$

Bethe-Bloch formula

Consider particle of charge ze , passing a stationary charge Ze



Assume

- Target is non-relativistic
- Target does not move

Calculate

- Energy transferred to target (separate)

Bethe-Bloch formula

Force on projectile

$$F_x = \frac{Zze^2}{4\pi\epsilon_0 r^2} \cos \theta = \frac{Zze^2}{4\pi\epsilon_0 b^2} \cos^3 \theta$$

Change of momentum of target/projectile

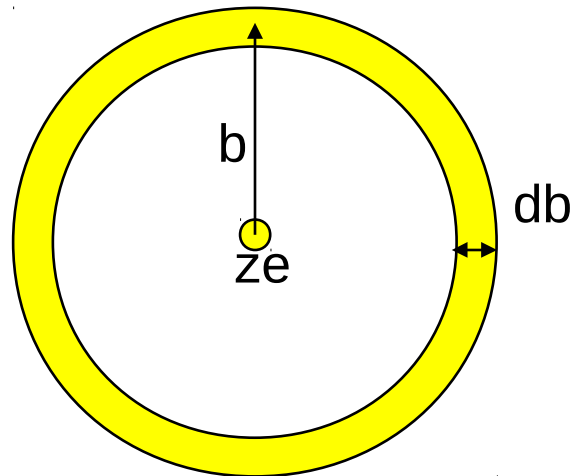
$$\Delta p = \int_{-\infty}^{\infty} dt F_x = \frac{Zze^2}{2\pi\epsilon_0 \beta c} \frac{1}{b}$$

Energy transferred

$$\Delta E = \frac{\Delta p^2}{2M} = \frac{Z^2 z^2 e^4}{2M (2\pi\epsilon_0)^2 (\beta c)^2} \frac{1}{b^2}$$

Bethe-Bloch formula

- Energy transfer is determined by impact parameter b
- Integration over all impact parameters:



$$\frac{dn}{db} = 2\pi b \times (\text{number of electrons / unit area})$$

$$= 2\pi b \times Z \frac{N_A}{A} \rho \Delta x$$

Bethe-Bloch formula

Calculate average energy loss

$$\begin{aligned}\overline{\Delta E} &= \int_{b_{\min}}^{b_{\max}} db \frac{dn}{db} E_e(b) = 2C \frac{m_e c^2}{\beta^2} \frac{Z z^2}{A} \rho \Delta x [\ln b]_{b_{\min}}^{b_{\max}} \\ &= C \frac{m_e c^2}{\beta^2} \frac{Z z^2}{A} \rho \Delta x [\ln E]_{E_{\min}}^{E_{\max}}\end{aligned}$$

$$\text{with } C = 2\pi N_A \left(\frac{e^2}{4\pi\epsilon_0 m_e c^2} \right)$$

There must be limit for E_{\min} and E_{\max} :

- All the physics and material dependence is in the calculation of this quantities

Bethe-Bloch formula

Simple approximations:

From relativistic kinematics

$$E_{\max} = \frac{2\gamma^2 \beta^2 m_e c^2}{1 + 2\gamma \frac{m_e}{M} + \left(\frac{m_e}{M}\right)^2} \approx 2\gamma^2 \beta^2 m_e c^2$$

Inelastic collision

$E_{\min} = I_0 \equiv$ average ionisation energy

Resulting formula:

$$\frac{\overline{\Delta E}}{\Delta x} \approx 2C \frac{m_e c^2}{\beta^2} \frac{Z z^2}{A} \rho \ln \left(\frac{2\gamma^2 \beta^2 m_e c^2}{I_0} \right)$$

Bethe-Bloch formula

$$-\frac{dE}{dx} = \left(\frac{e}{4\pi\epsilon_0} \right)^2 \frac{4\pi (ze)^2 n}{m_0 c^2 \beta^2} \left[\ln \frac{2m_0 c^2 \beta^2}{I} - \ln(1 - \beta^2) - \beta^2 \right]$$

incoming particle: β : v/c
v: velocity
ze: charge

absorber material: n: electron density (electrons/cm³)
I: average excitation and ionisation potential
 $\sim 10 Z$ eV

electron: e: charge
 m_0 : rest mass

Bethe-Bloch formula

$$-\frac{dE}{dx} = \left(\frac{e}{4\pi\epsilon_0} \right)^2 \frac{4\pi (ze)^2 n}{m_0 c^2 \beta^2} \left[\ln \frac{2m_0 c^2 \beta^2}{I} - \ln(1 - \beta^2) - \beta^2 \right]$$

$$n \equiv N Z \equiv \frac{N_A \rho Z}{A}$$

N: atomic density (atoms/cm³)

Z: atomic number

N_A: Avogadro constant

ρ: density (g/cm³)

A: atomic weight

$$-\frac{dE}{dx} = 0.31 \text{ MeV cm}^2 \frac{z^2 \rho Z}{\beta^2 A} \left[\ln \frac{2m_0 c^2 \beta^2}{I} - \ln(1 - \beta^2) - \beta^2 \right]$$

Stopping power dependencies

non-relativistic Bethe-Bloch

$$-\frac{dE}{dx} = \left(\frac{e}{4\pi\epsilon_0} \right)^2 \frac{4\pi (ze)^2 n}{m_0 v^2} \left[\ln \frac{2m_0 v^2}{I} \right]$$

[...] changes slowly

$$-\frac{dE}{dx} \propto \mu \frac{z^2 n}{v^2}$$

different energy

$$-\frac{dE}{dx} \propto \mu \frac{1}{v^2} \propto \mu \frac{1}{E}$$

different particle
(same velocity)

$$-\frac{dE}{dx} \propto \mu z^2$$

different material

$$-\frac{dE}{dx} \propto \mu n$$

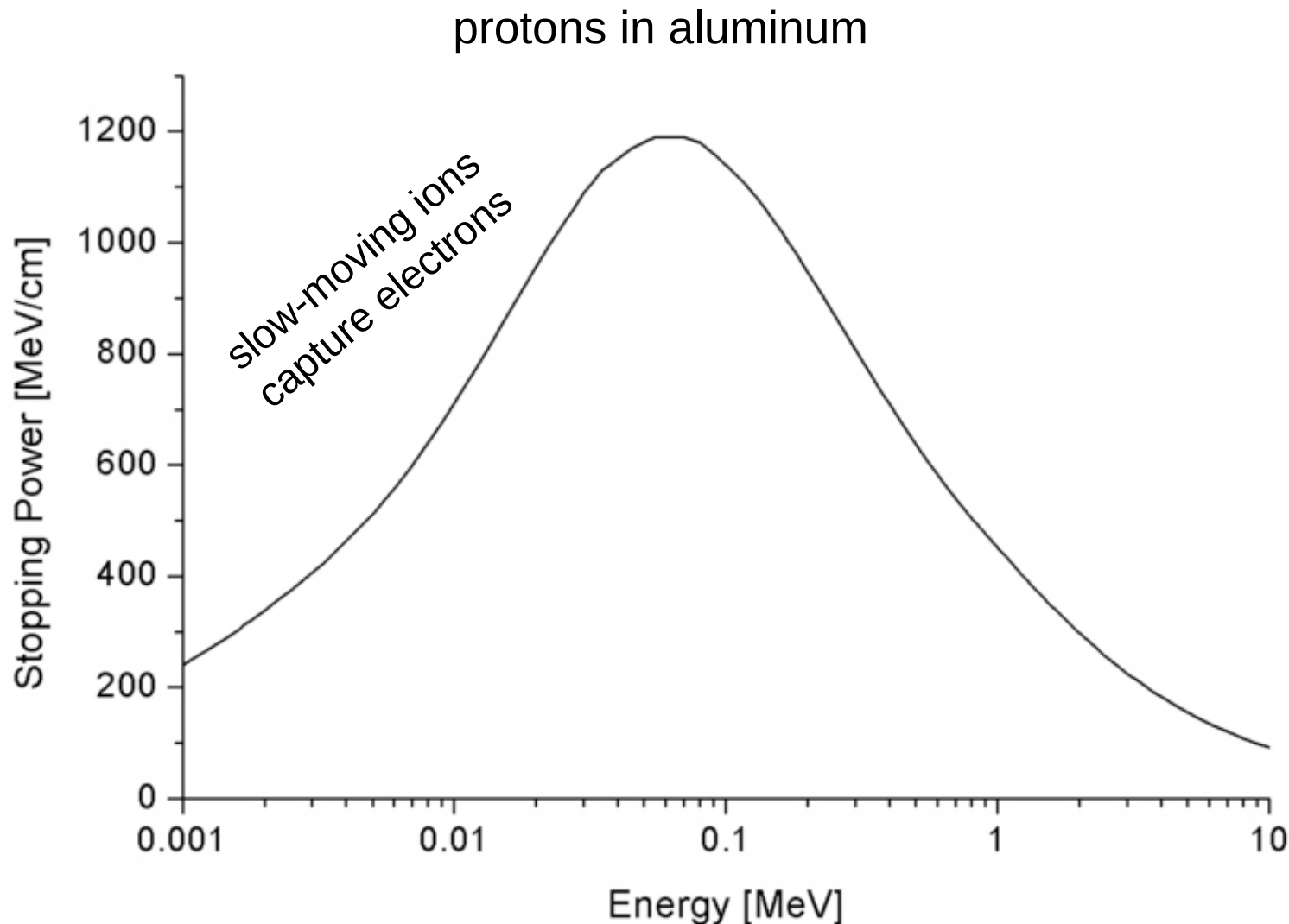
Bragg-Kleeman rule

stopping power per atom of compounds/mixtures is additive

$$\frac{1}{N_c} \left(\frac{dE}{dx} \right)_c = \sum_i W_i \frac{1}{N_i} \left(\frac{dE}{dx} \right)_i$$

N_c, N_i : atomic density of compound, component
 W_i : atomic fraction of component i

Stopping power example #1



Stopping power example #2

G.F. Knoll, *Radiation Detection and Measurement*, 3rd Edition

about same energy loss minima
→ minimum ionizing particle
~2 MeV/(g/cm²) in light materials

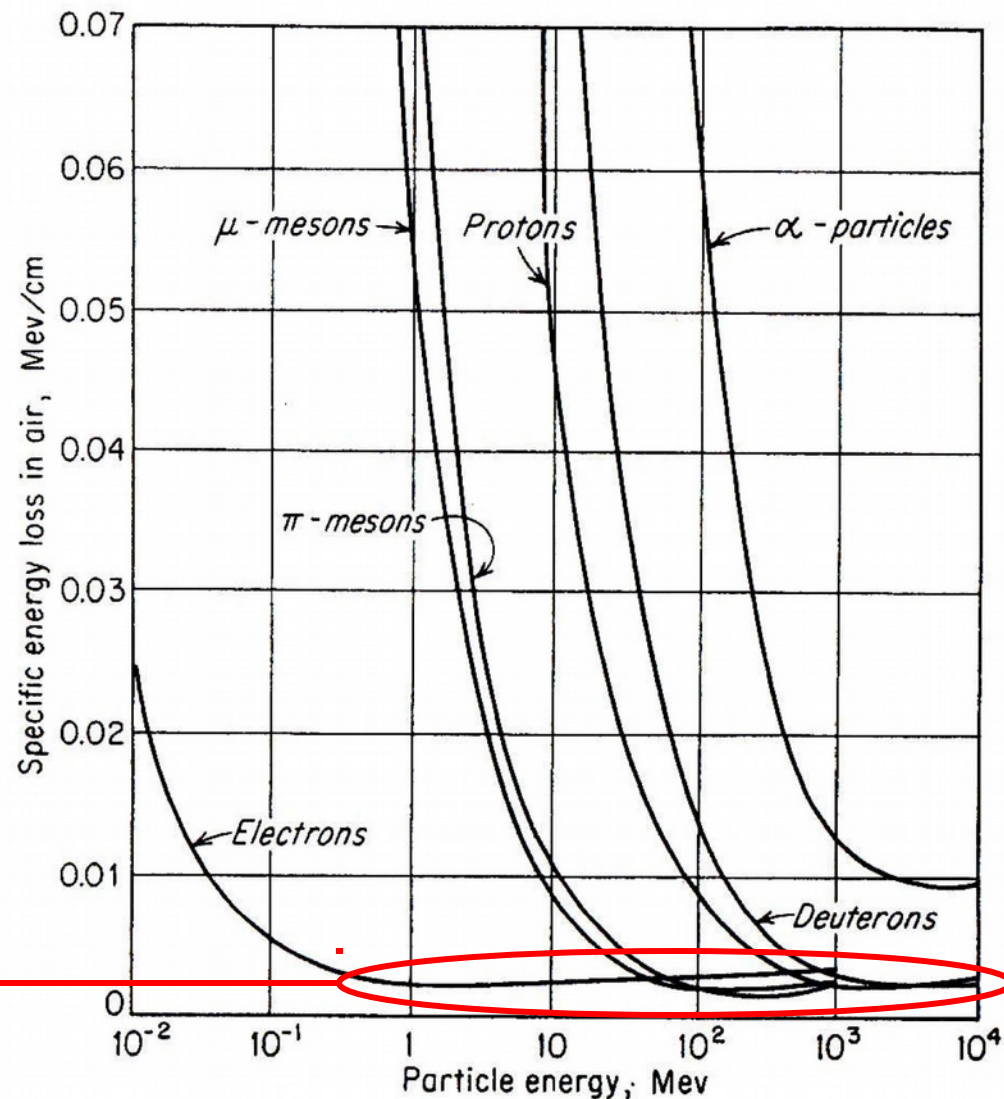
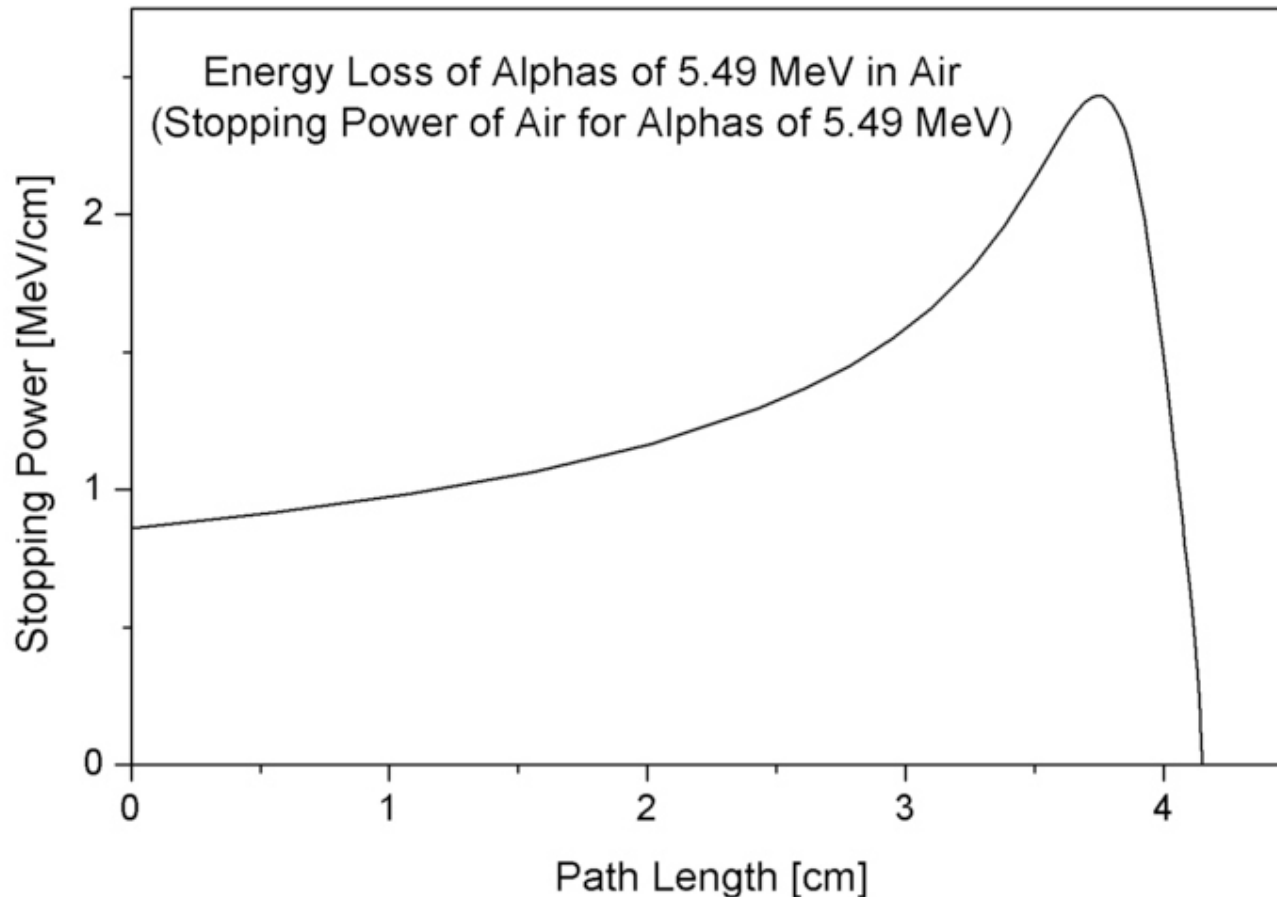


Figure 2.1 Variation of the specific energy loss in air versus energy of the charged particles shown. (From Beiser.²)

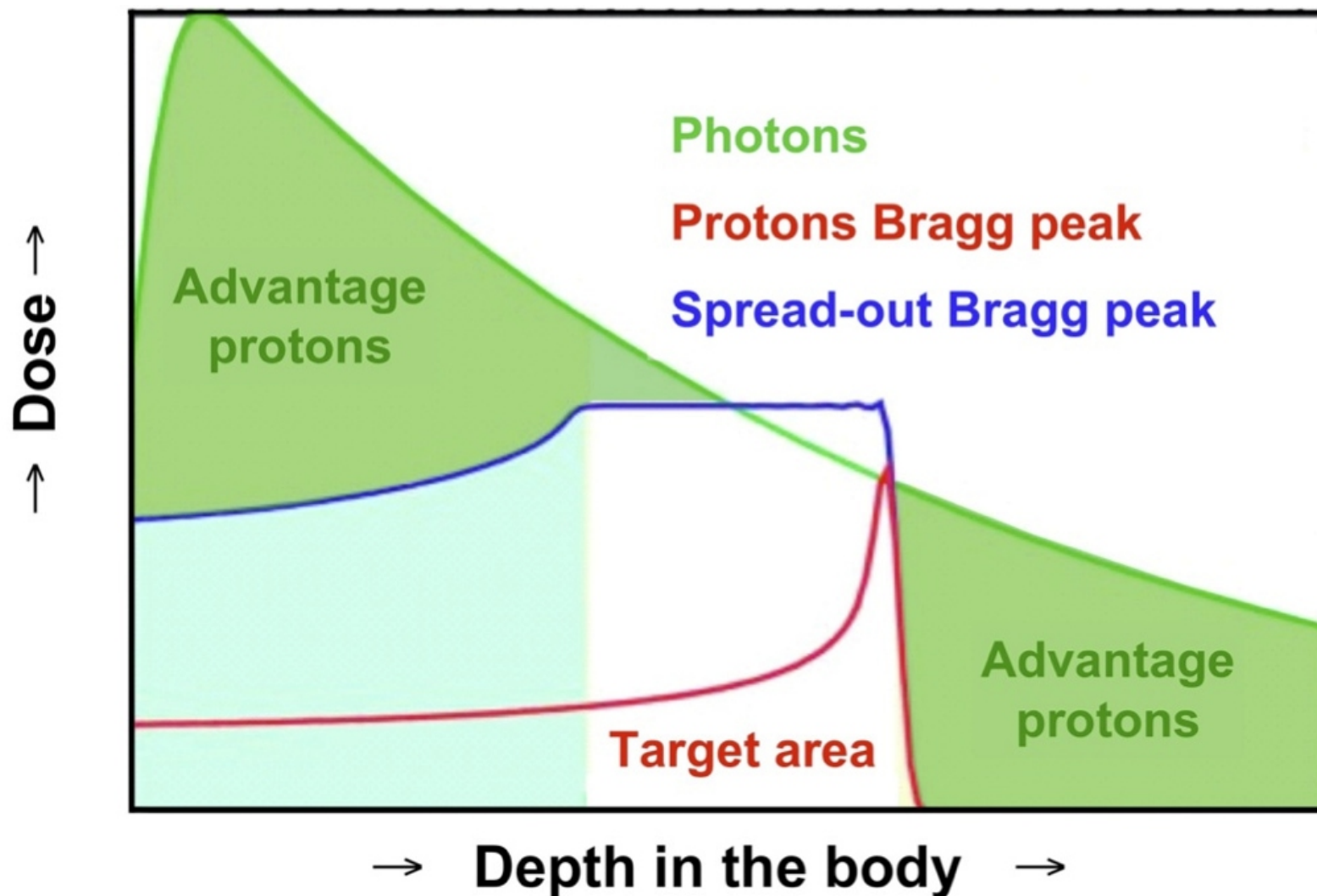
The Bragg peak

stopping power vs. distance travelled



basis for hadron (e.g. proton) therapy

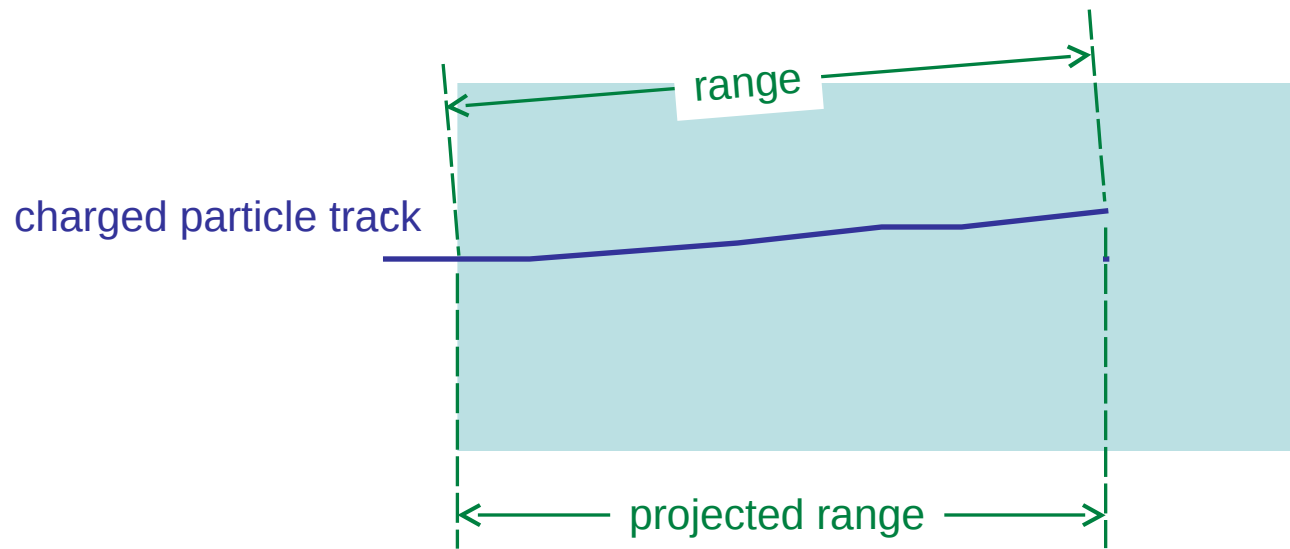
Photon vs. proton radiation therapy



Range of a charged particle

≡ distance travelled before stopping

$$R = \int_{E_0}^0 \left(-\frac{dE}{dx} \right)^{-1} dE$$



of more practical use: projected range
(= “range”)

Electrons

electron mass is small

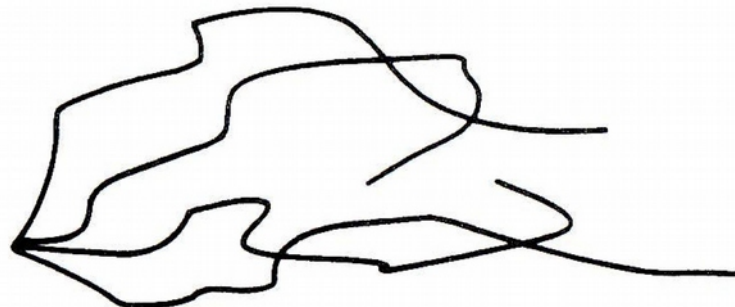
→ Coulomb interaction causes:

- large relative energy loss per interaction
- large deviations in path

→ large accelerations cause energy loss
due to electromagnetic radiation: bremsstrahlung

→ distance travelled \gg projected range

→ backscattering (low E and high Z)



Electron energy loss

$$\frac{dE}{dx} = \left(\frac{dE}{dx} \right)_C + \left(\frac{dE}{dx} \right)_R$$

c: collisional
r: radiative

$$-\left(\frac{dE}{dx} \right)_C = \left(\frac{e}{4\pi\epsilon_0} \right)^2 \frac{2\pi e^2 n}{m_0 c^2 \beta^2} \left[\ln \frac{m_0 v^2 E}{2I^2(1-\beta^2)} - (\ln 2) \left(2\sqrt{1-\beta^2} - 1 + \beta^2 \right) + (1-\beta^2) + \frac{1}{8} \left(1 - \sqrt{1-\beta^2} \right)^2 \right]$$

$$-\left(\frac{dE}{dx} \right)_R = \left(\frac{e}{4\pi\epsilon_0} \right)^2 \frac{e^2 n (Z+1) E}{137 m_0^2 c^4} \left[4 \ln \frac{2E}{m_0 c^2} - \frac{4}{3} \right]$$

$$\frac{(dE/dx)_r}{(dE/dx)_c} \cong \frac{E_{[\text{MeV}]} Z}{700}$$

Electron collisional vs. radiative energy loss

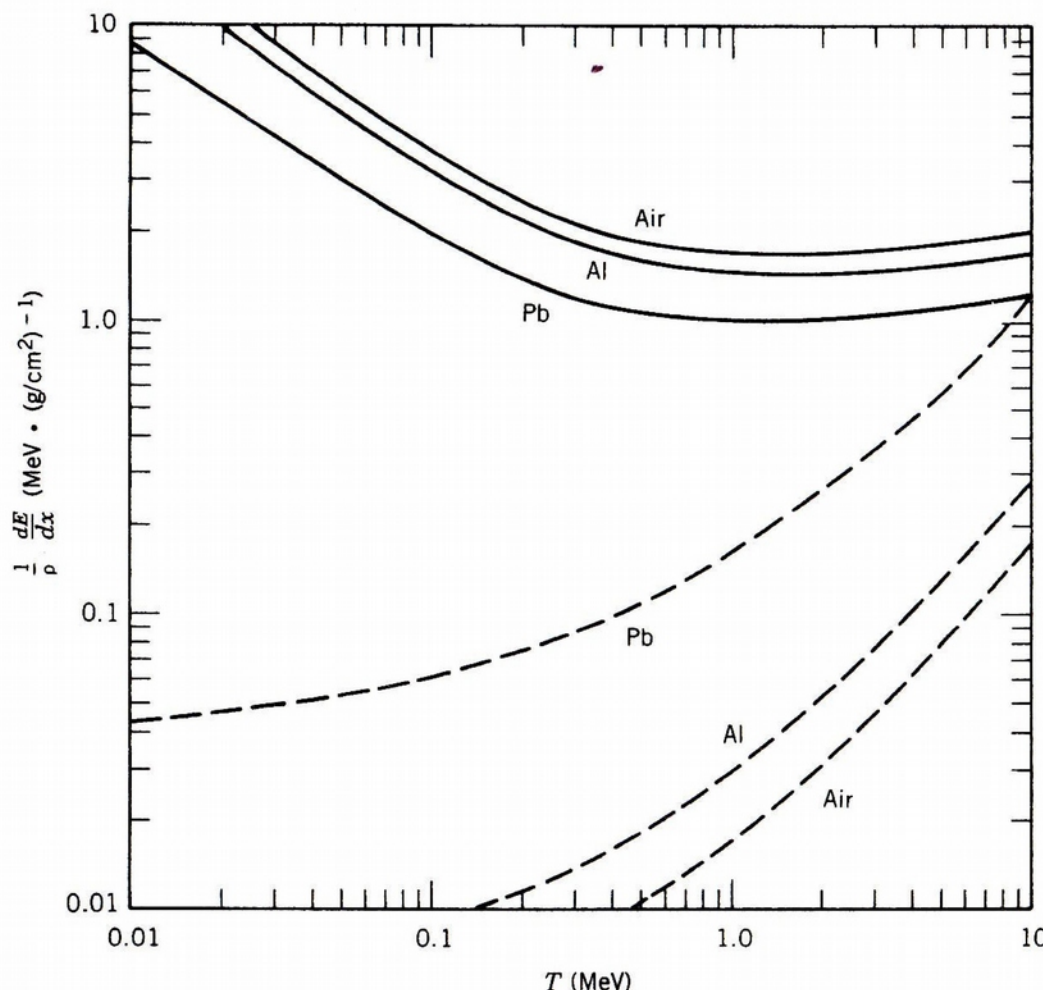


Figure 7.3 Energy loss by electrons in air, Al, and Pb. To suppress the large variation in dE/dx arising from the number of electrons of the material, the quantity $\rho^{-1}(dE/dx)$ is plotted. Solid lines are for collisions; dashed lines are for radiation. For additional tabulated data on energy losses, see L. Pages et al., *Atomic Data 4*, 1 (1972).

Electron stopping power

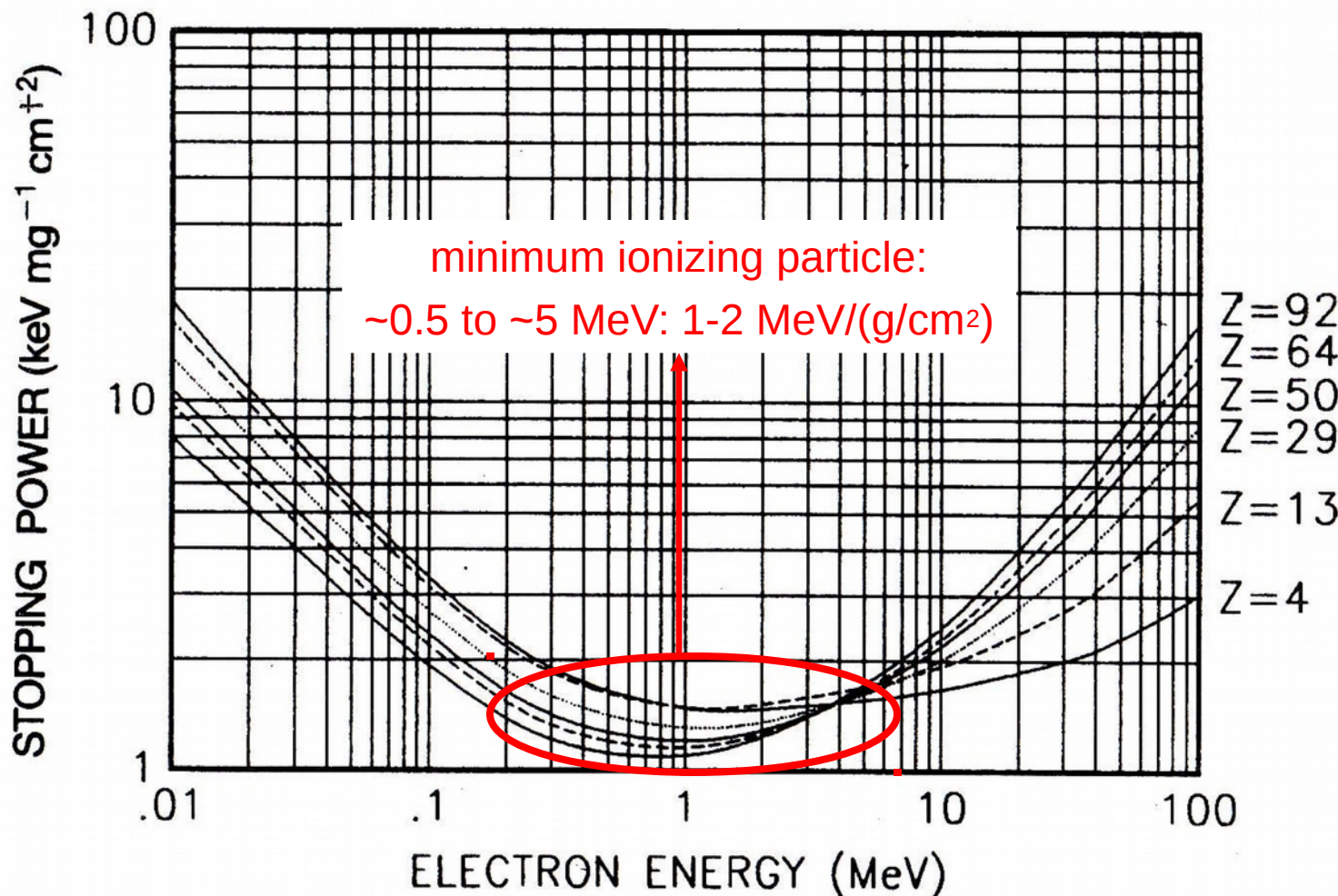


Figure 7-10 Stopping power of electrons in the energy range from 0.01 MeV to 100 MeV for a number of elements. For low- Z substances, dE/dx is almost constant between about 0.5 MeV and several MeV. The rise of the curves at high energies is due to increasing bremsstrahlung probability.

Stopping high-energy electrons

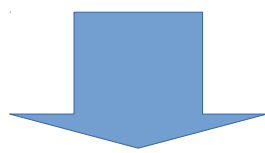
Interactions of a high-energy electron includes:

- Energy loss due to bremsstrahlung (extra photon is created):

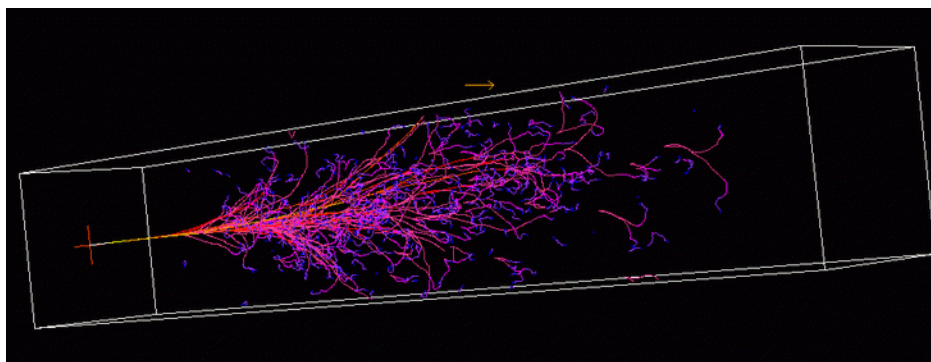
Radiation length mean distance over which the electron energy is reduced to 1/e of its original value due to radiation loss only

$$X_0 = \frac{A \cdot 716.4 \text{ g} \cdot \text{cm}^{-2}}{Z \cdot (Z + 1) \cdot \ln(287 / \sqrt{Z})}$$

- Generated photons have high energy → will be converted into e^+e^- pairs



Shower of particles will be generated:
EM shower



Stopping high-energy electrons

Interactions of a high-energy electron includes:

- Energy loss due to bremsstrahlung (extra photon is created):

Radiation length mean distance over which the electron energy is reduced to 1/e of its original value due to radiation loss only

$$X_0 = \frac{A \cdot 716.4 \text{ g} \cdot \text{cm}^{-2}}{Z \cdot (Z + 1) \cdot \ln(287 / \sqrt{Z})}$$

The mean free path of a high energy photon for pair production is 9/7 of a radiation length

The Moliere radius is a good scaling variable for describing the transverse dimension of an electromagnetic shower

$$R_M = 0.0265 \cdot X_0(Z + 1.2)$$



X₀ – characteristic scale to calculate dimensions of a detector

Straggling

energy loss is a stochastic process

→ energy straggling

→ range straggling

→ angular straggling

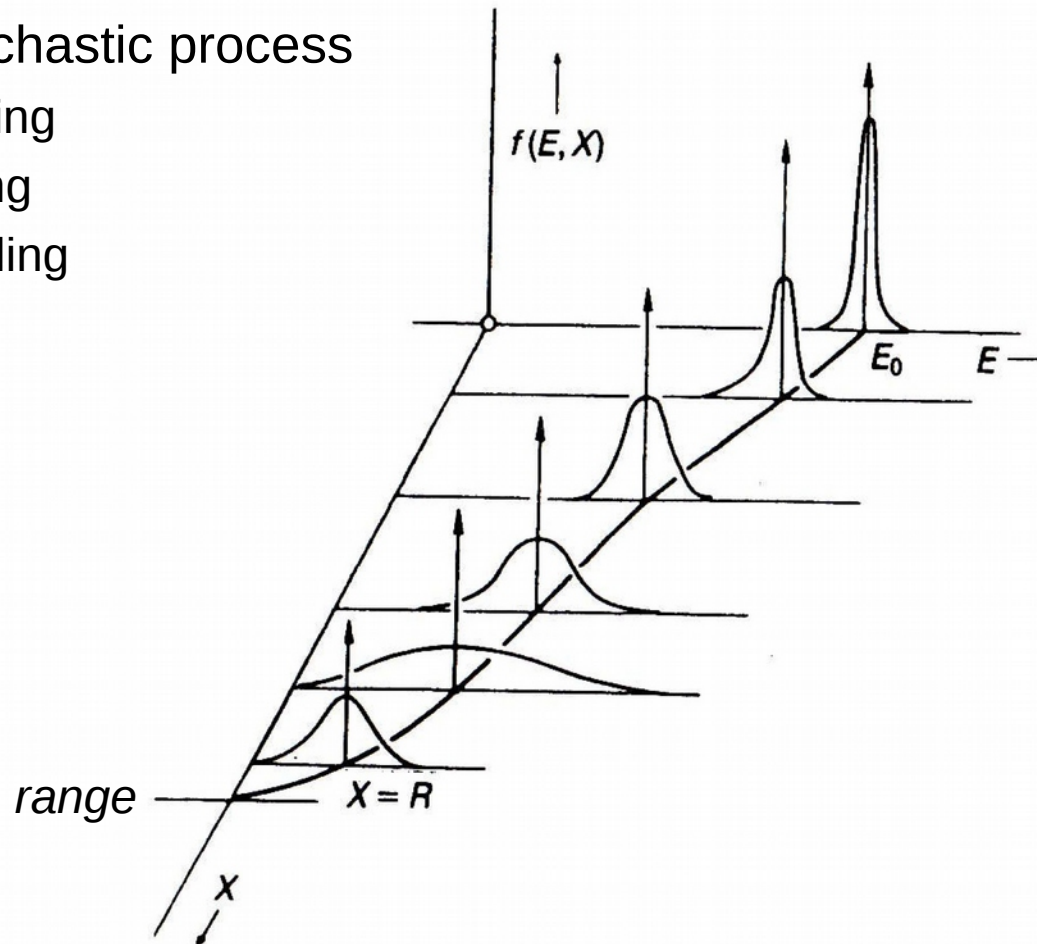


Figure 7-24 Behaviour of the energy distribution $f(E, X)$ of initially monoenergetic charged particles at various penetration distances. E is the particle energy and X the distance along the path. Observe the decrease of energy along the route; the low-energy tail is most clearly seen in the first distribution curve inside the stopping substance.

Range example: hydrogen, helium ions

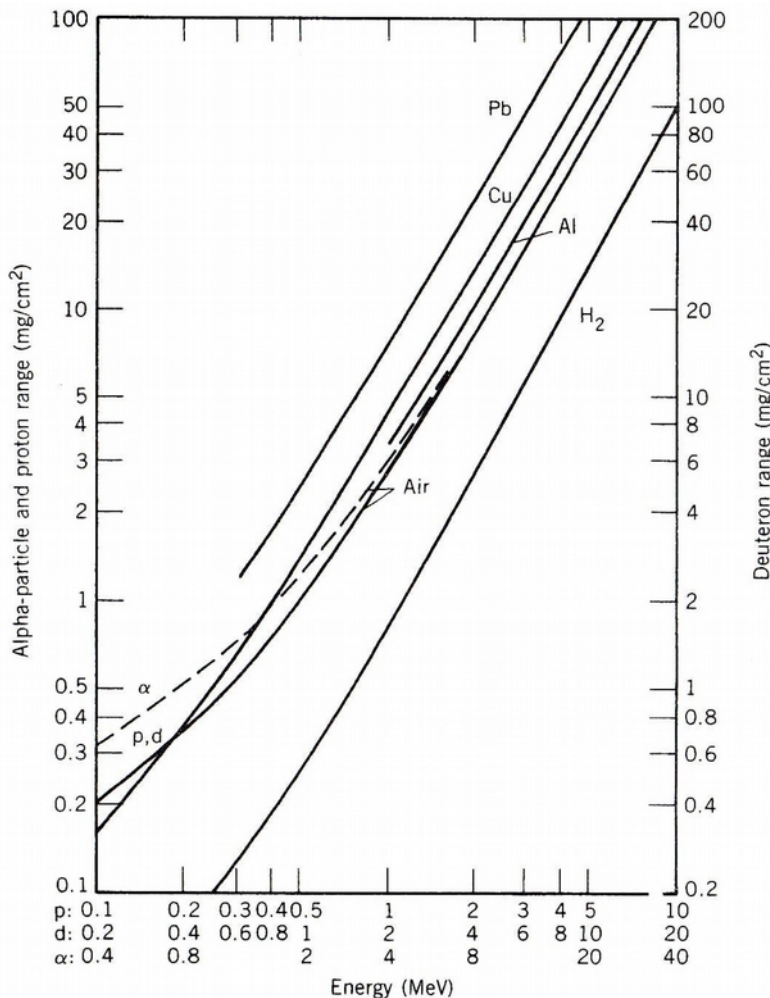


Figure 7.2 The range-energy relationship in various materials. Because the particles lose energy through scattering by atomic electrons, the range depends inversely on the density. It is therefore convenient to plot the product range \times density, in units of mg/cm^2 . Unfortunately, this product is also called “range” in the literature. From A. H. Wapstra et al., *Nuclear Spectroscopy Tables* (Amsterdam: North-Holland, 1959).

Electron range: examples

G.F. Knoll, *Radiation Detection and Measurement*, 3rd Edition

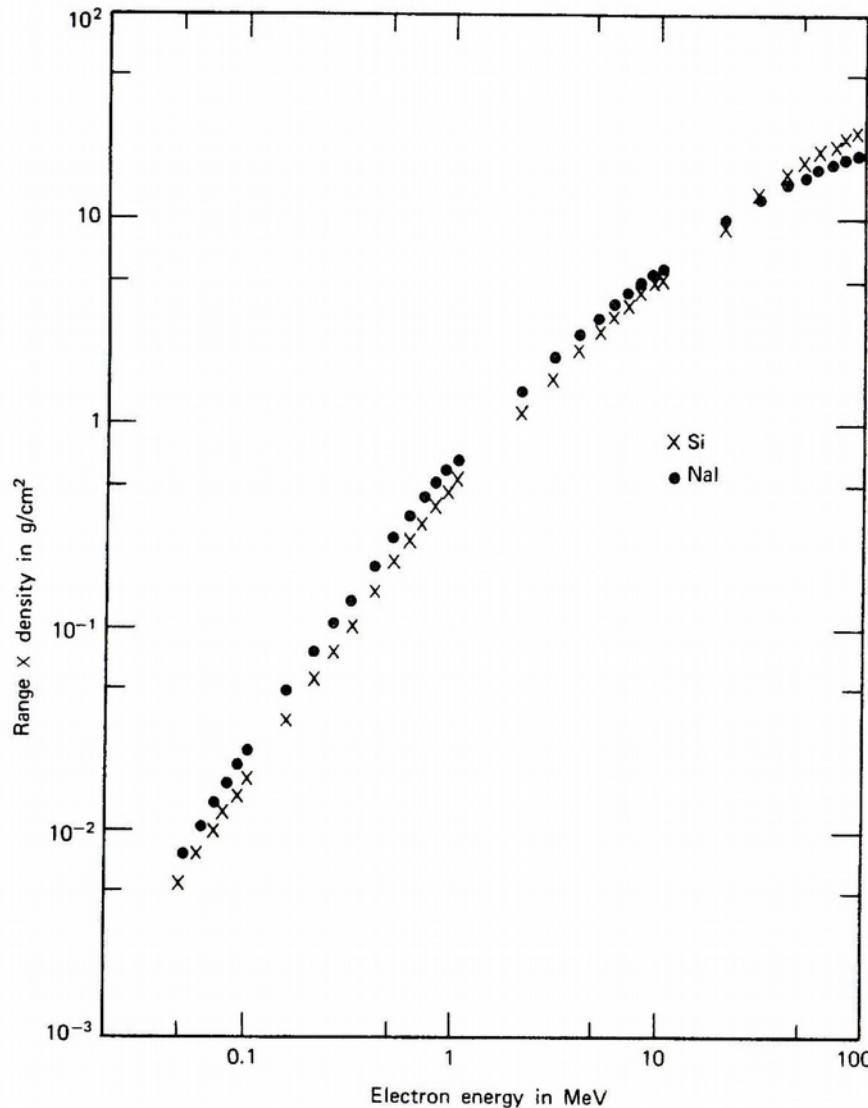


Figure 2.14 Range–energy plots for electrons in silicon and sodium iodide. If units of mass thickness (distance × density) are used for the range as shown, values at the same electron energy are similar even for materials with widely different physical properties or atomic number. (Data from Mukoyama.²⁴)

Electron range: examples

K.S. Krane, *Introductory Nuclear Physics*, 1st Edition

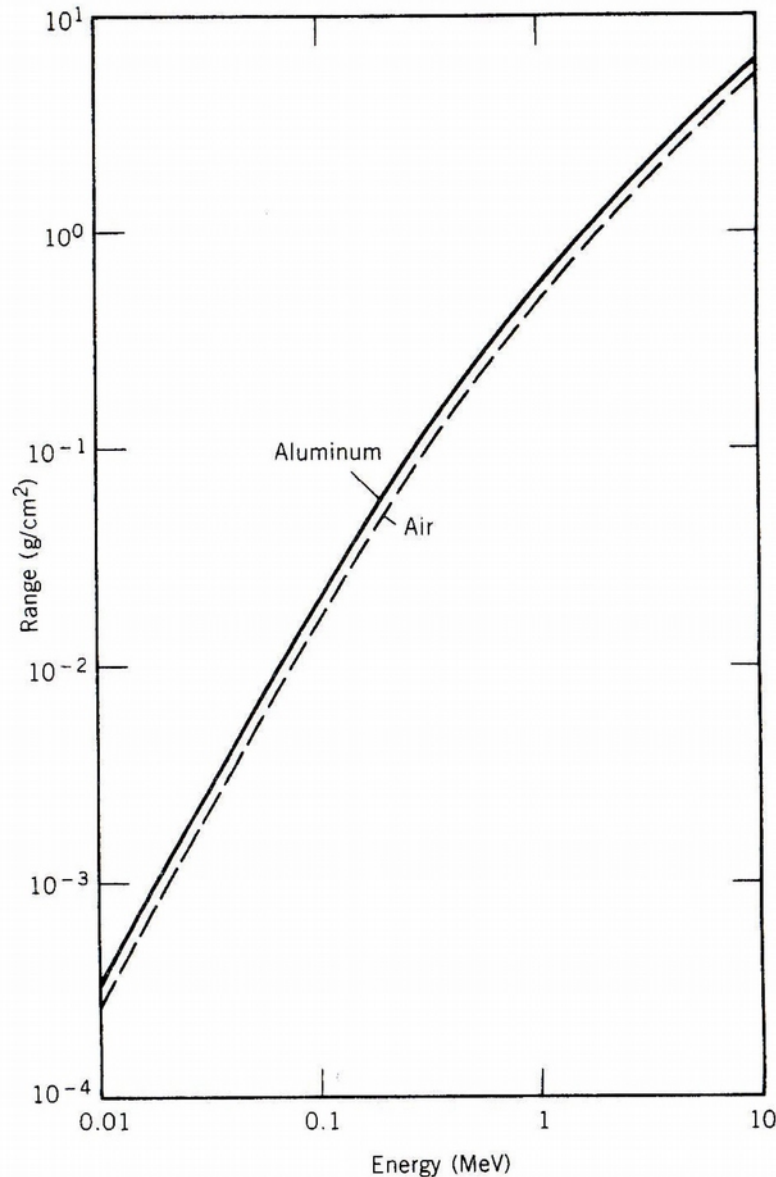


Figure 7.4 Range-energy relationship for electrons in air and in aluminum.

Cherenkov radiation (1/2)

- a charged particle travelling faster than the speed of light in a medium emits light, so-called Cherenkov radiation

$$v > \frac{c}{n}$$

$$\beta \equiv \frac{v}{c}$$

$$\beta n > 1$$

n: refractive index

- energy threshold

$$E_{th} = m_0 c^2 \left(-1 + \sqrt{1 + \frac{1}{n^2 - 1}} \right)$$

$m_0 c^2$: electron rest mass



Cherenkov threshold energy

G.F. Knoll, *Radiation Detection and Measurement*, 3rd Edition

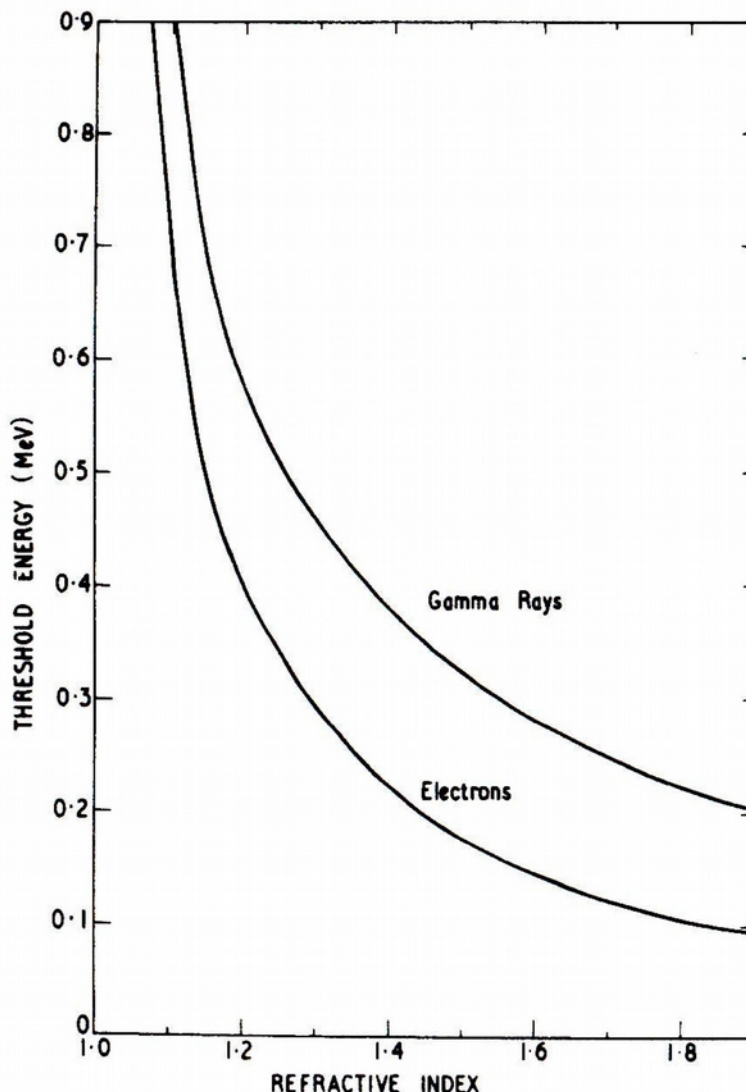
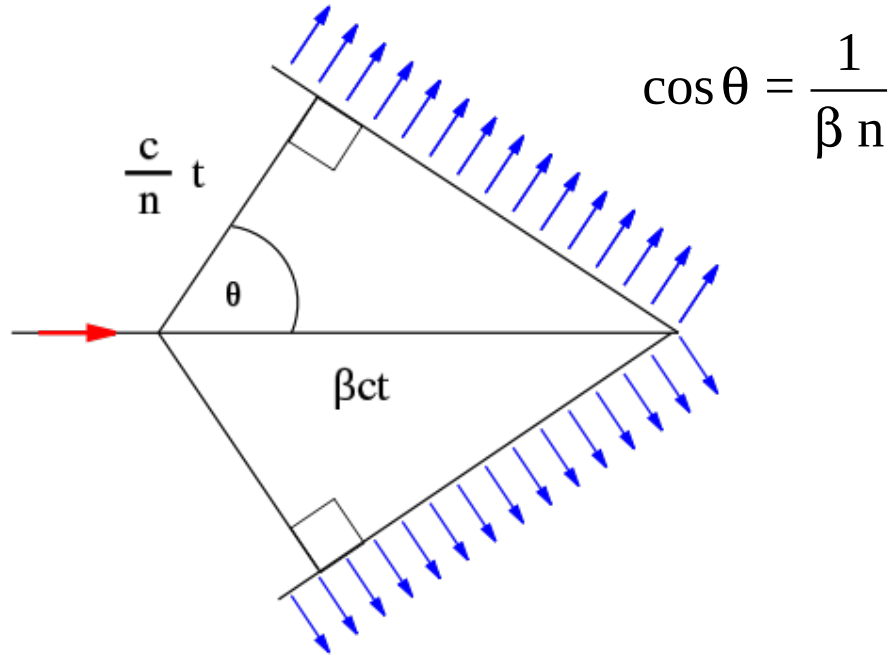


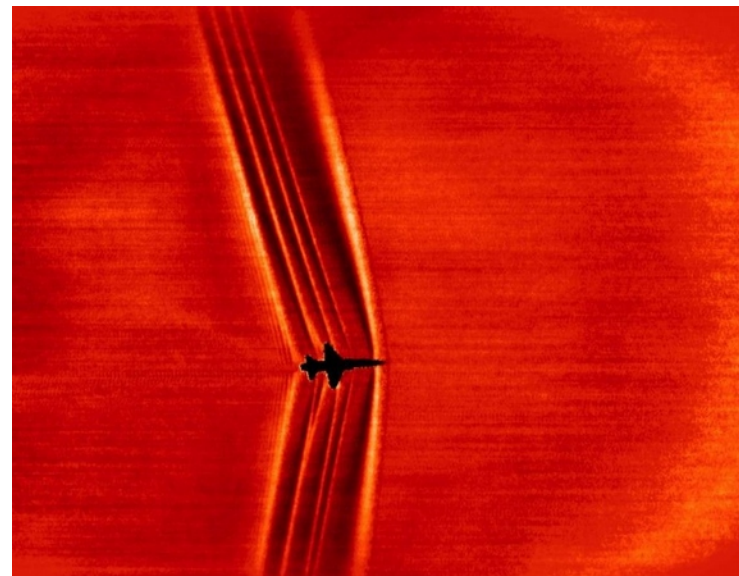
Figure 19.1 The threshold energy for Cherenkov radiation as a function of the index of refraction of the detection medium. Curves are shown both for electrons and for gamma rays that can yield, by 180° Compton scattering, an electron of the threshold energy. (From Sowerby.²)

Cherenkov radiation (2/2)

- Cherenkov photons are emitted under a fixed angle



Photograph of a super-sonic jet air-plane



- yield per unit wavelength $\propto 1/\lambda^2$
(breaks down at short λ as $n \rightarrow 1$)

NASA

Cherenkov light yield

$$\frac{d^2N}{dE dx} \approx 370 z^2 \sin^2\theta(E) \quad \frac{1}{eV} \frac{1}{cm}$$

ze: charge of particle

G.F. Knoll, *Radiation Detection and Measurement*, 3rd Edition

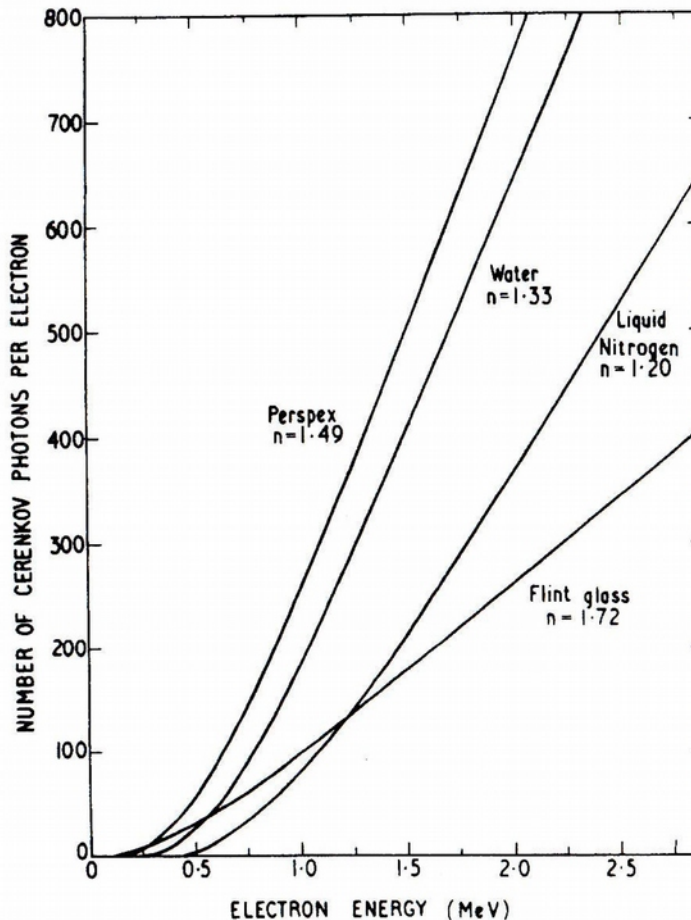
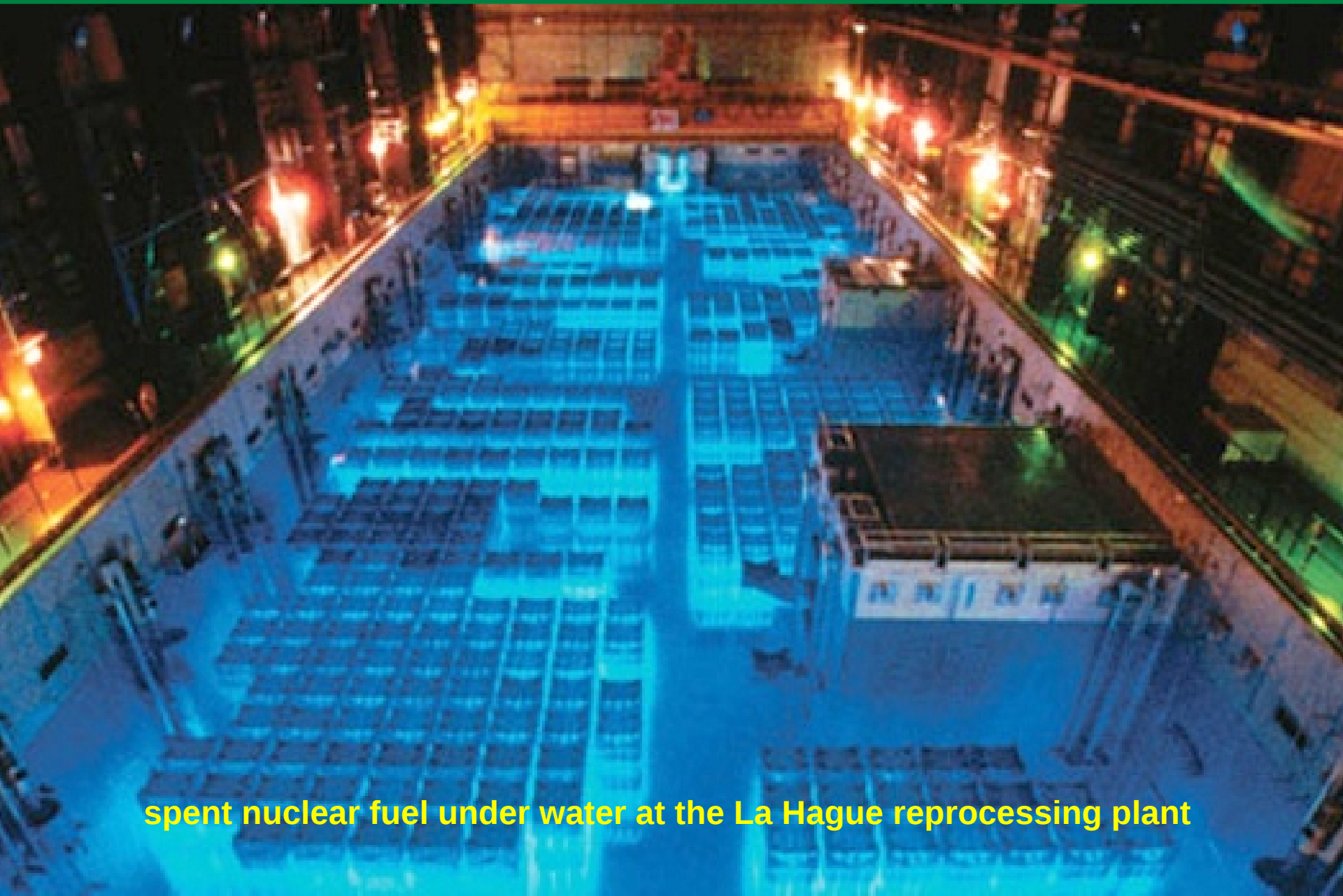


Figure 19.2 Calculated yield of Cherenkov photons in the 300–600 nm wavelength region for several detection media. (From Sowerby.²)

Cherenkov radiation: example



spent nuclear fuel under water at the La Hague reprocessing plant

Neutrons

- no Coulomb interaction, only strong interaction
 - short range & atomic nucleus is small:
 - interaction probability << than charged particles/photons ($\sim 10^8$)
 - as the result of an interaction:
 - neutron disappears, creating secondary radiation
 - mostly heavy charged particles (p,d,t, α) (basis for detection)
 - scattering in which energy and direction are significantly changed
 - can give rise to recoil nuclei (basis for detection)
- attenuation of a collimated beam is exponential

Neutrons

type of interaction depends mostly on the neutron energy

- fast neutrons ($> \sim 0.5$ eV)
 - elastic scattering (most effective on light nuclei), gives recoil nuclei
 - inelastic scattering, gives recoil nuclei
 - scattering results in neutron energy loss (neutron is moderated)
 - neutron capture (resulting in the emission of charged particles (p, d, t, α))
 - resonant
- slow neutrons
 - elastic scattering
 - small energy loss, so not good for detection, but thermalizes neutrons (~25 meV at room temperature)
 - eventually captured by nucleus followed by gamma ray: (n, γ)
 - most effectively by B, Cd, In, Gd

Neutrinos

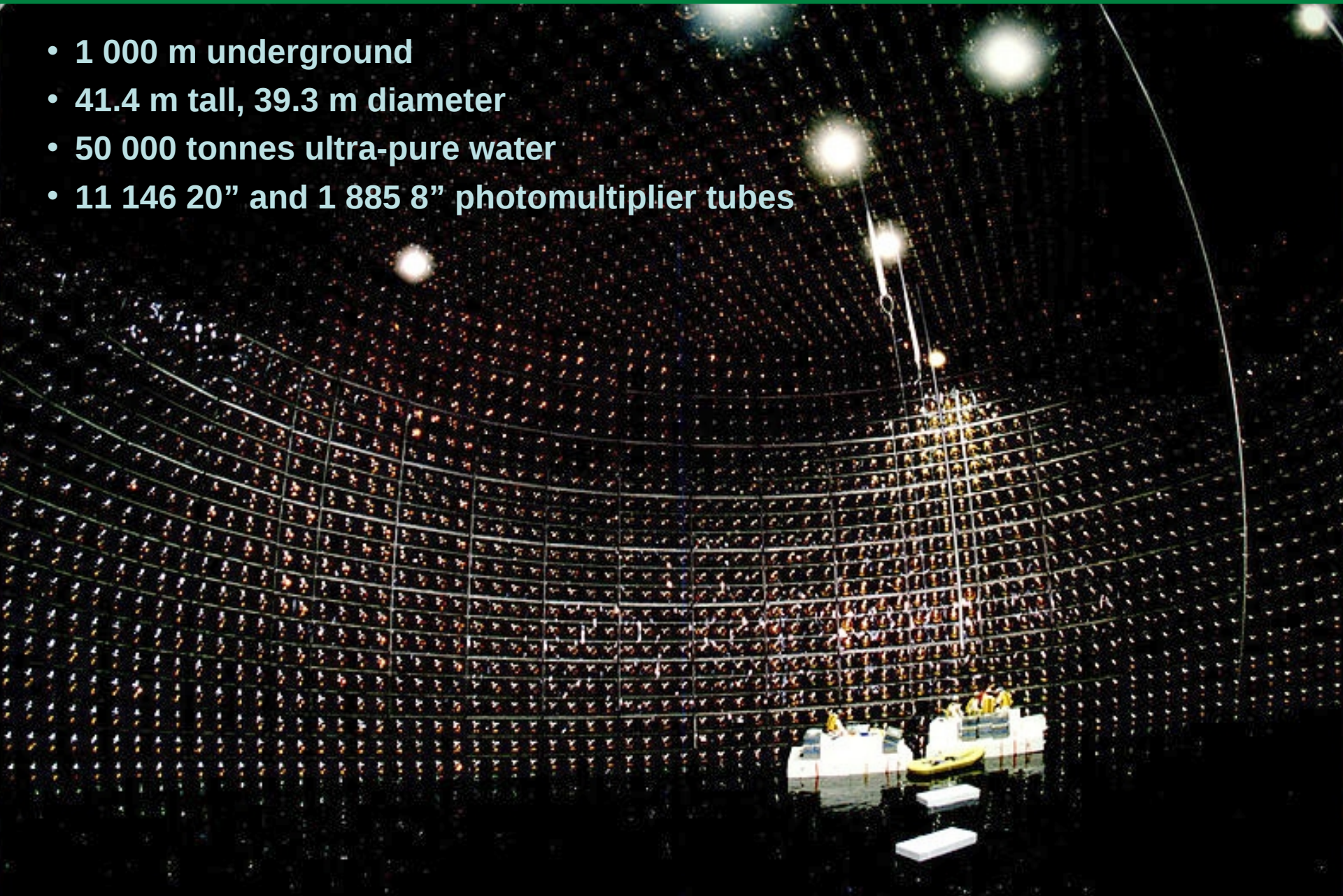
- no electromagnetic or strong interaction, only weak interaction
→ very small interaction probability
 - e.g. $\bar{\nu}_e + p \rightarrow n + e^+$ cross section $\sim 10^{-43} \text{ cm}^2$
 - 1 cm³ of material contains $\sim 10^{24}$ protons
 - interaction probability $\sim 10^{-43} \times 10^{24} \sim 10^{-19} / \text{cm}$
 - 10^{19} cm (10 light-years) required for a good capture probability
- neutrino interaction results in secondary radiation, which is then detected
- interaction possibilities and probabilities are different for the 3 neutrino flavours: electron-, muon-, and tau-neutrino

Neutrino detection schemes

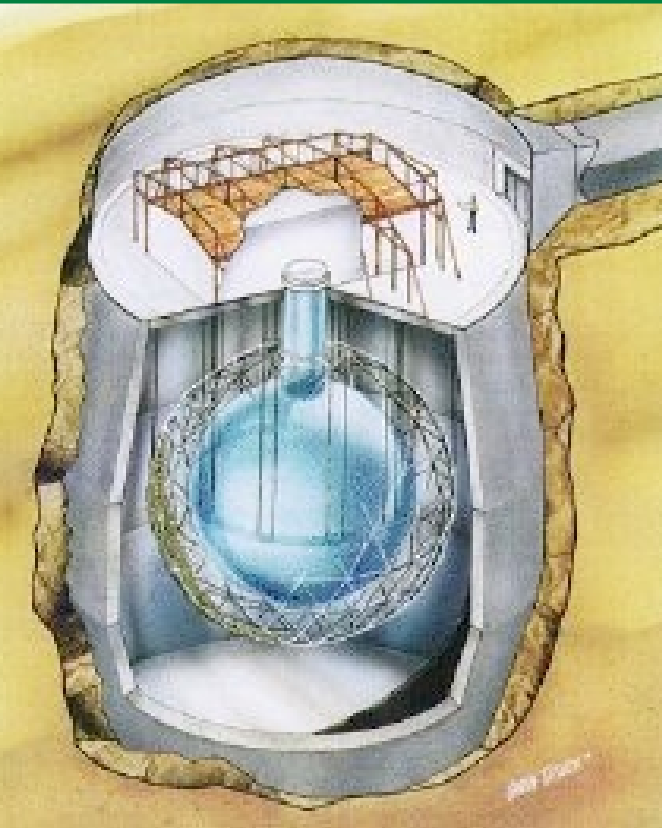
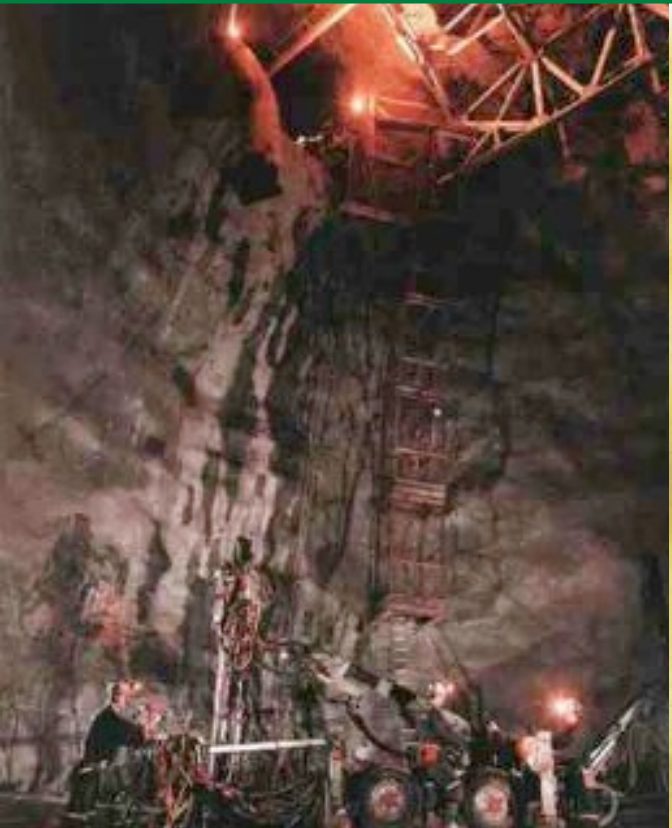
- inverse beta-decay
 - $\bar{\nu}_e + {}_Z^A X \rightarrow e^+ + {}_{Z-1}^A Y$ detect e^+ (annihilation) and/or Y (radiochemical detection)
- neutrino capture by a nucleus (Homestake experiment)
 - $\nu_e + {}_{17}^{37} Cl \rightarrow e^- + {}_{18}^{37} Ar$ detection of ${}_{18}^{37} Ar$
- water-Cherenkov detection: scattering off electrons $\nu + e^- \rightarrow \nu + e^-$
 - all neutrino flavours but with different cross sections
 - detected via Cherenkov radiation from the scattered electrons ($E_\nu > 5$ MeV)
 - Cherenkov cone tells incoming direction and particle type
 - e.g. (Super)-Kamiokande
- heavy water: 3 options, all 3 neutrino flavours can be distinguished
 - scattering off electrons (all 3 flavours, different cross sections)
 - $\nu_e + d \rightarrow p + p + e^-$ detect e^- via Cherenkov, only ν_e
 - $\nu + d \rightarrow \nu + n + p$ deuteron break-up, detect neutron, all 3 flavors, same cross section
 - e.g. SNO (Sudbury Neutrino Observatory)

Super-Kamiokande

- 1 000 m underground
- 41.4 m tall, 39.3 m diameter
- 50 000 tonnes ultra-pure water
- 11 146 20" and 1 885 8" photomultiplier tubes



Sudbury Neutrino Observatory



- **2 km underground**
- **1 000 tonnes of heavy water**
- **6-metre radius acrylic vessel**
- **9 600 photomultiplier tubes**